# Phosphole-Containing π-Conjugated Systems: From Model Molecules to Polymer Films on Electrodes

Caroline Hay,[a] Muriel Hissler,[a] Cédric Fischmeister,[a] Joëlle Rault-Berthelot,[b]
Loïc Toupet,[c] László Nyulászi,*[d] and Régis Réau*[a]

*Dedicated to Professor Robert Weiss on the occasion of his 60th birthday*

**Abstract:** Two series of 2,5-dipyridyl- and 2,5-dithienylphosphole derivatives containing $\sigma^3$- or $\sigma^4$-P atoms were prepared, and their optical (UV/Vis absorption, fluorescence spectra) and electrochemical properties were systematically evaluated. These physical properties depend mainly on the natures of the 2,5-substituents and of the phosphorus moiety, and they revealed that these compounds contain extended π-conjugated systems. Structure–property relationships were established on the basis of these experimental data and ab initio calculations on the parent molecules. The limited aromatic character and low-lying LUMO of the phosphole ring appear to be crucial for achieving a highly delocalised π system. Electrooxidation of 2,5-dithienylphosphole derivatives affords electroactive films with low optical band gaps. As observed for the corresponding monomers, the optical and electrochemical properties of the polymers can be varied over a wide range by modifying the nature of the phosphorus moiety.

**Keywords:** ab initio calculations · electrochemistry · phosphorus heterocycles · pi interactions · thin films

## Introduction

Linear π-conjugated oligomers and polymers based on a planar backbone of $sp^2$-bonded carbon atoms have attracted increasing interest in recent years owing to their potential application in electronic devices (e.g., light-emitting diodes, thin-film transistors, photovoltaic cells).[1] The optical and electronic properties of these macromolecules depend significantly on their HOMO–LUMO gap and the electron density of the carbon backbone. Several strategies have been developed to vary these parameters with the aim of preparing novel conjugated frameworks with enhanced performance. A common approach for tuning the properties of *p*-phenylenevinylenes, which are the best studied conjugated polymers, is to introduce lateral substituents with specific electronic and/or steric properties.[1a] Another successful strategy involves the incorporation of aromatic heterocycles in the backbone of π-conjugated systems.[1d–2] The possibility of incorporating heterocyclic building blocks with different aromatic character and electronic nature allows for engineering at the molecular level. Indeed, low aromaticity favours electron delocalisation along the main chain, while maximum conjugation is obtained in copolymers with alternating electron-rich and electron-deficient subunits due to intramolecular charge transfer (ICT).[2a–d] Heterocyclopentadienes have been extensively used for such purposes, since their electronic properties depend on the nature of the heteroatoms. For example, metalloles of Group 14 elements (siloles, germoles, stannoles) exhibit a high electron affinity,[2i–l] whereas those of Groups 15 (pyrrole) and 16 (furan, thiophene) have electron-rich aromatic π-systems.[2f]

Although the chemistry of phospholes is well developed,[3] these phosphacyclopentadienes have received little attention as building blocks for π-conjugated systems. Mathey et al. reported the synthesis of well-defined oligophospholes **A**[4a] and α-thienyl-α-phospholes **B**[4b,c] (Figure 1). X-ray diffraction studies show that these oligomers exhibit significant rotational disorder that prevents extended π-conjugation.[4d] Tilley et al. recently described the first polymer containing phosphole rings **C** (Figure 1).[4e] Due to their irregular structure (2,4-

---

[a] Prof. R. Réau, C. Hay, Dr. M. Hissler, Dr. C. Fischmeister
Organométalliques et Catalyse
Chimie et Electrochimie Moléculaires
UMR 6509. CNRS-Université de Rennes 1
Institut de Chimie de Rennes, Campus de Beaulieu
35042 Rennes Cedex (France)
Fax: (+33) 2-99-28-69-39
E-mail: regis.reau@univ-rennes1.fr

[b] Dr. J. Rault-Berthelot
Laboratoire d'Electrochimie Moléculaire et Macromoléculaire
UMR 6510. CNRS-Université de Rennes 1
Institut de Chimie de Rennes
Campus de Beaulieu, 35042 Rennes Cedex (France)

[c] Dr. L. Toupet
Groupe Matière Condensée et Matériaux
UMR 6626, CNRS-Université de Rennes 1, Campus de Beaulieu
35042 Rennes Cedex (France)

[d] Dr. L. Nyulászi
Departement of Inorganic Chemistry
Technical University of Budapest
1521 Budapest Gellért tér 4 (Hungary)
Fax: (+36) 1463-3363
E-mail: nyulaszi.inc@chem.bme.hu

0947-6539/01/0719-4222 $ 17.50+.50/0

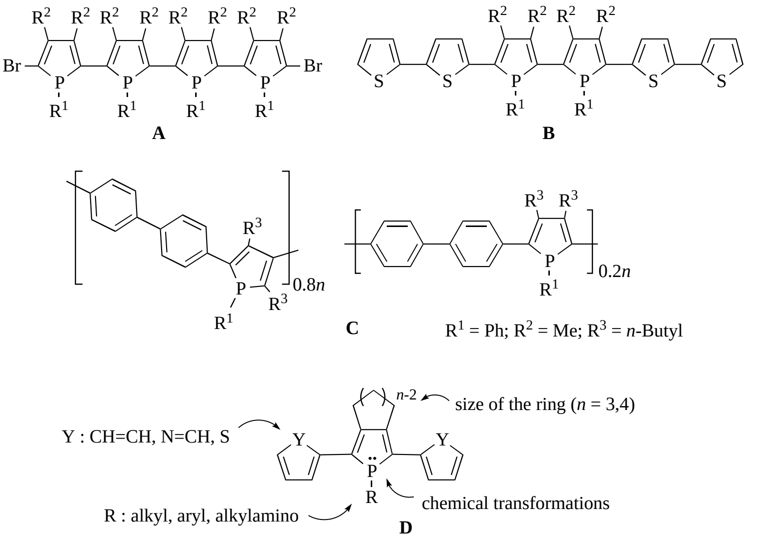

Figure 1. Known phosphole-containing oligomers **A** and **B** and polymers **C**. General structure of 2,5-diarylphosphole **D**.

and 2,5-linkages) these polymers have relatively wide HOMO–LUMO gaps and are efficient emitters of blue light. The scarcity of such materials is surprising, since phospholes have certain properties that make them attractive synthons for the construction of π-conjugated systems.[5a,b] The phosphorus atom does not readily form sp hybrids and mainly employs p electrons for bonding. This leads to a pyramidal geometry of the tricoordinate phosphorus atom and a pronounced s character of the lone pair.[3, 5] These geometric and electronic features prevent efficient interaction of the lone pair on phosphorus with the endocyclic diene system. Hence, phospholes possess 1) a weak aromatic character, which should favour delocalisation of the π-system, and 2) a reactive heteroatom, which potentially offers the possibility of tuning the HOMO and the LUMO levels by chemical modification. These properties prompted us to prepare a family of 2,5-diaryl- and 2,5-diheteroarylphosphole derivatives **D** (Figure 1) as model compounds. Several strategic structural variations can be envisaged for tuning their electronic properties and elucidating structure–property relationships. Electron-deficient 2-pyridyl or electron-rich 2-thienyl substituents can be introduced at the 2,5-positions of the phosphole ring; the size of the fused carbocycle and the substituents on phosphorus can also be varied. Finally, chemical modification of the nucleophilic P atom can be performed.

Here we report on full details of the chemistry of compounds **D**, including crystal structures, UV/Vis absorption and fluorescence data, electrochemical behaviour and theoretical calculations. The electropolymerisation of 2,5-bis(2-thienyl)phosphole derivatives and the electrochemical and spectroscopic characterisation of the resulting materials are also presented.

## Results

**Synthesis of 2,5-diheteroaryl- and 2,5-diarylphospholes**: The target phospholes **D** were prepared by the Fagan–Nugent route,[6] a classical and efficient method for heterole synthesis.[2g–i, q, 3] The intramolecular oxidative coupling of diynes **1**, which contain a $(CH_2)_3$ or a $(CH_2)_4$ spacer to facilitate the desired 2,5-substitution pattern, with "zirconocene" gave the corresponding zirconacyclopentadienes **2** (Scheme 1). To gain more insight into the properties of the key organometallic intermediates **2**,[2g–i] zirconacyclopentadienes **2a** (45% yield) and **2b** (63% yield) bearing 2-pyridyl and 2-thienyl units, respectively (Scheme 1), were isolated as extremely air- and moisture-sensitive red crystalline solids.[7, 8a] Complexes **2a**,**b** were characterised by NMR spectroscopy in solution. The nature of the 2,5-substituents has an influence on the $^{13}C$ NMR chemical shifts of the C atoms of the metallacycle. Compound **2a**, which bears electron-withdrawing 2-pyridyl groups, has signals at lower field than those of bis(2-thienyl)-substituted **2b**. This effect is more pronounced for the C atoms in the β-position with respect to the metal centre ($C_\alpha$: **2a**: $\delta = 179.8$, **2b**: $\delta = 177.9$; $C_\beta$: **2a**: $\delta = 153.5$, **2b**: $\delta = 142.1$). Complex **2b**, which is also a key intermediate for the preparation of bis(2-thienyl)metalloles[2i] and -thiophene oxides,[2g] was subjected to an X-ray structure analysis (Figure 2, Tables 1 and 2), which revealed a twisted arrangement, with torsion angles of 41.0 and 40.5° between the thiophene units and the slightly puckered

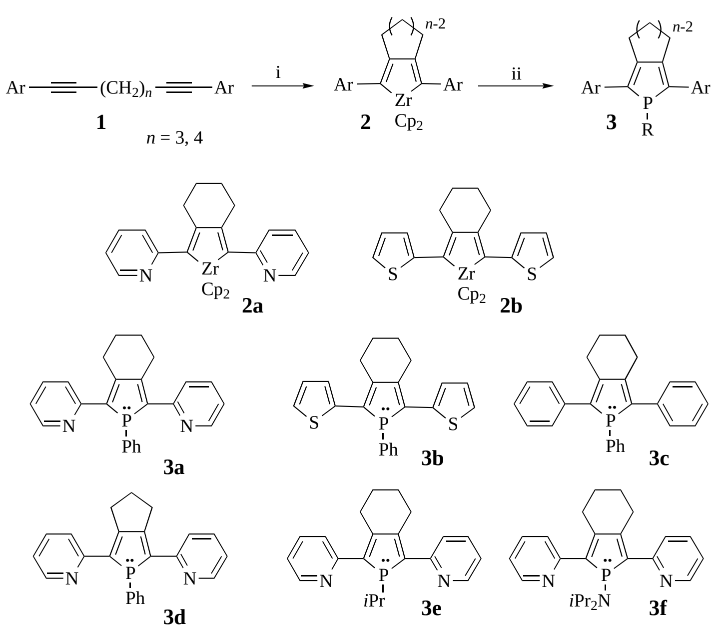

Scheme 1. Synthesis of 2,5-diheteroaryl- and 2,5-diarylphospholes **3**. i) $[Cp_2ZrCl_2]$, nBuLi (2 equiv), THF, −78 °C to RT, 12 h; ii) $PhPX_2$, THF, −78 °C to RT/40 °C, 3–5 h.

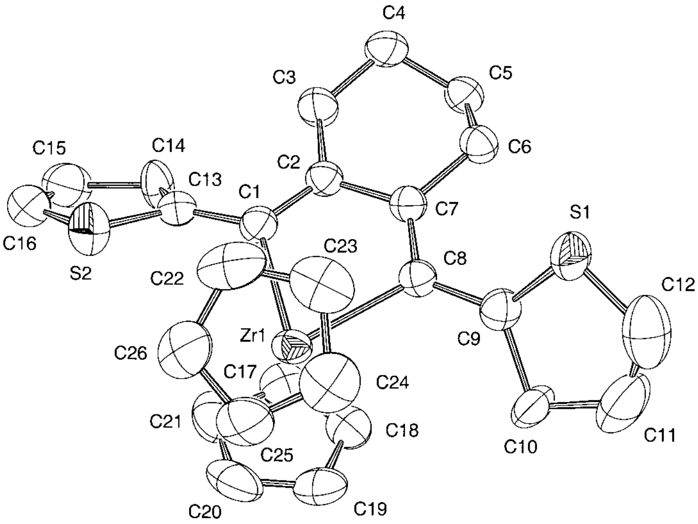

Figure 2. Molecular structure of complex **2b** in the solid state (50% probability thermal ellipsoids) with atom labelling for Table 1 (hydrogen atoms omitted for clarity).

Table 1. Selected bond lengths [Å] and angles [°] for zirconacyclopentadiene **2b**, phospholes **3a**,[9a] **3b**[9b] and complexes **7a**[9a] and **7b**.

| | **2b**[a] | **3a**[b] | **3b**[b] | **7a**[c] | **7b**[c] |
|---|---|---|---|---|---|
| M–C1 | 2.255(4) | 1.806(6) | 1.817(4) | 1.820(5) | 1.821(8) |
| M–C8 | 2.269(4) | 1.806(6) | 1.818(5) | 1.819(4) | 1.817(8) |
| C1–C2 | 1.353(6) | 1.365(9) | 1.366(6) | 1.356(5) | 1.357(11) |
| C2–C7 | 1.494(6) | 1.478(9) | 1.465(7) | 1.466(8) | 1.487(11) |
| C7–C8 | 1.340(6) | 1.354(8) | 1.356(6) | 1.352(5) | 1.349(11) |
| C1–C13 | 1.471(7) | 1.466(9) | 1.436(6) | 1.463(7) | 1.449(10) |
| C8–C9 | 1.466(6) | 1.467(8) | 1.457(6) | 1.461(7) | 1.457(10) |
| C1-M-C8 | 76.4(2) | 90.5(3) | 90.9(2) | 90.5(2) | 91.4(4) |
| M-C8-C7 | 112.6(3) | 110.7(5) | 110.2(4) | 110.0(4) | 110.0(6) |
| C7-C2-C1 | 118.5(4) | 113.8(6) | 114.9(4) | 113.9(4) | 114.5(7) |
| C2-C1-M | 112.9(3) | 110.7(4) | 109.3(3) | 110.3(4) | 109.3(6) |
| C1-M-C17 | – | 103.2(3) | 104.3(2) | 105.2(2) | 103.7(3) |
| C8-M-C17 | – | 105.4(3) | 104.1(2) | 103.3(2) | 104.3(4) |

[a] M = $ZrCp_2$. [b] M = PPh. [c] M = $PW(CO)_5Ph$.

zirconacyclopentadiene ring (C2-C7-C8-Zr 3.6(5), C7-C2-C1-Zr 7.3(5)°). These inter-ring twist angles are far larger than those recorded for Group 14 bis(2-thienyl)metalloles (6.0–16.5°)[2i] and thiophene oxides (11.2 and 26.3°).[2g] The endocyclic C-Zr-C and Zr-C-C angles, as well as the Zr–C bond lengths, are unremarkable[8] (Table 1) and reveal no constraints imposed by the fused carbocycle.[8a]

Addition of $PhPCl_2$ to a solution of **2a** in THF at room temperature cleanly afforded phosphole **3a**. In contrast, **2b** is inert toward $PhPCl_2$, but reacts with $PhPBr_2$ to give phosphole **3b** in nearly quantitative yield. Phospholes **3a**,**b** can be obtained in higher overall yields in a one-pot procedure which avoids the isolation of **2a**,**b** (Table 3).[9a,b] Phospholes **3d** and **3e** (Scheme 1) were obtained in moderate yields by using this one-pot procedure; yields of **3c** and **3f** were lower (Table 3). The dipyridyl-, dithienyl- and diphenylphospholes exhibit comparable stability towards hydrolysis and oxidation both in solution (THF, $CH_2Cl_2$) and in the solid state. In fact, the stability of these phospholes is directly related to the nature of the *P*-substituent. 1-Phenylphospholes **3a**–**d** can be isolated by flash column chromatography on basic alumina as air-stable solids. In contrast, 1-alkylphosphole **3e** can only be handled under an inert atmosphere, while 1-aminophosphole **3f** is extremely air and moisture sensitive and decomposes during purification. The solid-state thermal stability was determined by thermogravimetric analysis and differential scanning calorimetry under a nitrogen atmosphere. Here again, the *P*-phenyl- and *P*-alkylphospholes **3a**–**e** are most stable and decompose (5% loss of weight) only above 200 °C (Table 3).

Compounds **3a**–**e** were characterised by high-resolution mass spectrometry and gave satisfactory elemental analyses. Solid-state structures were determined for **3a**[9a] and **3b**[9b] (vide infra). The multinuclear NMR data of compounds **3a**–**f** are consistent with the proposed structures (Table 3). The NMR data of phospholes **3a**,**b** were independent of temperature between +80 and −60 °C, and the simplicity of the $^{13}C$ NMR spectra favours symmetrical structures. However, a statistical disorder (*syn*,*syn*/*anti*,*anti* arrangement 20:80) was observed in the solid state for **3b** (vide infra). Furthermore, theoretical calculations predict a low energy barrier to rotation about the inter-ring C–C bonds (vide infra). It is thus very likely that this dynamic process is rapid in solution.

It is well established that any correlations between the $^{13}C$ NMR data for the endocyclic $C_\alpha$ and $C_\beta$ atoms (i.e., chemical shifts, $J_{PC}$ coupling constants) and the extent of cyclic

Table 2. Data for the structure determination of **2b** and **7b**.

| | **2b** | **7b** |
|---|---|---|
| formula | $C_{26}H_{24}S_2Zr$ | $C_{27}H_{19}O_5PS_2W$ |
| $M_r$ | 491.79 | 702.36 |
| $T$ [K] | 293 | 293 |
| crystal system | monoclinic | triclinic |
| space group | $P2_1/c$ | $P\bar{1}$ |
| $a$ [Å] | 9.7556(3) | 10.010(5) |
| $b$ [Å] | 12.2638(4) | 11.348(7) |
| $c$ [Å] | 18.7421(6) | 13.734(5) |
| $\alpha$ [°] | 90 | 75.93(3) |
| $\beta$ [°] | 99.481(2) | 70.21(3) |
| $\gamma$ [°] | 90 | 64.14(6) |
| $V$ [Å$^3$] | 2211.69(11) | 1312.6(11) |
| $Z$ | 4 | 2 |
| colour | red | pale yellow |
| crystal size [mm] | 0.36 × 0.21 × 0.20 | 0.40 × 0.35 × 0.33 |
| $\rho_{calcd}$ [Mg m$^{-3}$] | 1.477 | 1.777 |
| $F(000)$ | 1008 | 684 |
| $\mu$ ($Mo_{K\alpha}$) [cm$^{-1}$] | 6.96 | 46.56 |
| $\lambda$ [Å] | 0.71073 | 0.71073 |
| diffractometer | NONIUS Kappa CCD | CAD4 ENRAF-NONIUS |
| $h/k/l$ limits | 0;13/−16;17/−26;26 | 0;12/−13;14/−16;17 |
| scan range (2$\theta$) [°] | 3–60 | 3–54 |
| reflections collected/unique | 11973/4229 | 6061/5729 |
| $R$(int) | 0.0878 | 0.0328 |
| data with $I > 2\sigma(I)$ | 4229 | 4811 |
| data/restraints/parameters | 6456/0/263 | 5729/0/326 |
| goodness-of-fit on $F^2$ | 1.061 | 1.064 |
| final $R$ indices [$I > 2\sigma(I)$] $R1/wR2$ | 0.0773/0.2112 | 0.0627/0.1583 |
| $R$ indices (all data) $R1/wR2$ | 0.1187/0.2463 | 0.0787/0.1682 |
| largest diff. peak/hole [e Å$^{-3}$] | 1.446/−1.315 | 5.208/−3.689 |

Table 3. Selected NMR data,[a] yields[b] and Td$_5$[c] for phospholes **3a–f** and phosphole derivatives **5a,b–8a,b**.

| | $\delta$ $^{31}$P | $\delta$ $^{13}$C ($J_{\text{P-C}}$ [Hz]) C$\alpha$ | $\delta$ $^{13}$C ($J_{\text{P-C}}$ [Hz]) C$\beta$ | yield [%] | Td$_5$ [°C] |
|---|---|---|---|---|---|
| **3a** | +11.7 | 144.4 (4.6) | 148.1 (12.6) | 73 | 210 |
| **3b** | +12.7 | 135.7 (0) | 144.4 (9.0) | 75 | 205 |
| **3c** | +13.6 | 143.7 (2.4) | 144.2 (11.7) | 40 | 199 |
| **3d** | +36.0 | 139.6 (0) | 158.3 (10.2) | 70 | 197 |
| **3e** | +30.5 | 143.2 (0) | 147.0 (8.6) | 60 | 198 |
| **3f** | +45.3 | 144.4 (0) | 144.2 (12.6) | 23[d] | 182 |
| **4a** | +42.4 | – | – | 95[e] | – |
| **4b** | +42.3 | 125.0 (98.6) | 145.1 (24.2) | 95 | 214 |
| **5a** | +53.1 | 132.9 (83.0) | 152.1 (17.3) | 92 | 145 |
| **5b** | +52.6 | 128.5 (83.7) | 146.1 (20.9) | 93 | 253 |
| **6b** | +41.5 ($J_{\text{P-Se}}$ = 372.2 Hz) | 125.8 (74.3) | 145.6 (20.8) | 91 | 165 |
| **7a** | +30.2 ($J_{\text{P-W}}$ = 231.8 Hz) | 144.0 (45.0) | 148.3 (11.2) | 95 | 204 |
| **7b** | +33.4 ($J_{\text{P-W}}$ = 226.2 Hz) | 136.8 (43.5) | 144.2 (13.3) | 96 | 186 |
| **8a** | +41.4 | 128.6 (87.0) | 157.4 (20.4) | 75 | 148 |
| **8b** | +34.8 | 118.4 (85.3) | 154.1 (20.8) | 95 | 196 |

[a] Measured in CDCl$_3$ at 298 K. [b] Isolated yield, "one-pot" procedure. [c] Estimated by thermogravimetric analysis under N$_2$, 5% weight loss. [d] Compound **3f** can be obtained in 45% yield by subsequent addition of PCl$_3$ and *i*Pr$_2$NH. [e] According to NMR spectroscopy.

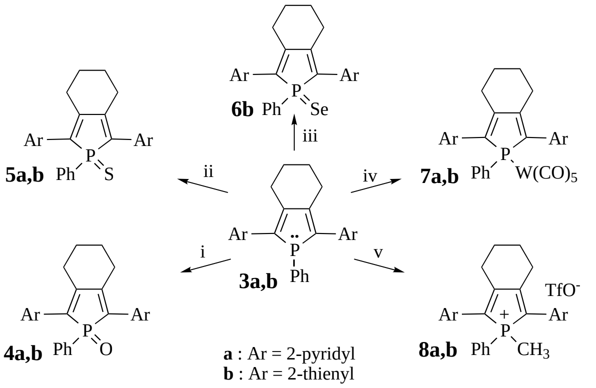

Scheme 2. Derivatisation of 2,5-diheteroarylphospholes **3a** and **3b**. i) Me$_3$SiOOSiMe$_3$, CH$_2$Cl$_2$, RT, 12 h; ii) 1/8 S$_8$, THF, RT, 36 h; iii) Se, THF, RT, 24 h; iv) [W(CO)$_5$(thf)], THF, RT, 3–15 h; v) MeOTf, RT, 12 h.

delocalisation within the phosphole ring are subjective and unconvincing.[3] The substitution pattern clearly has an impact on the NMR spectroscopic data of the phosphole ring, and the following features are noteworthy. As observed for the corresponding zirconacyclopentadienes **2a** and **2b**, the C$_\alpha$ and C$_\beta$ atoms of the pyridyl-substituted phosphole **3a** are more strongly deshielded than those of the corresponding dithienylphosphole **3b** (Table 3). The size of the fused carbocycle also has a marked influence. The $^{31}$P and $^{13}$C chemical shifts of **3a** with a 3,4-C$_4$ bridge are unremarkable (Table 3). In contrast, 3,4-C$_3$-bridged **3d** has a $^{31}$P NMR signal at an unusually low field [$\delta = +11.7$ (**3a**), $+36.0$ (**3d**)], and the chemical shifts of its C$_\alpha$ ($\delta = 139.6$) and C$_\beta$ atoms ($\delta = 158.3$) are more shielded and deshielded (**3a/3d**) than those of **3a** ($\delta = 144.4$ and 148.1), respectively. As was observed for other metalloles,[8a] this effect is probably associated with a modification of the angles within the phosphole ring due to the constraint imposed by the fused carbocycle. Finally, as is usually observed,[3] the $^{31}$P NMR chemical shifts of $\sigma^3,\lambda^3$-phospholes depend on the nature of the *P*-substituent. However, phospholes **3a**, **3e** and **3f** exhibit surprisingly similar $^{13}$C NMR data (Table 3).

**Derivatisation of 2,5-diheteroarylphospholes 3a and 3b**: The readily available phospholes **3a,b** were subjected to simple, classical reactions that exploit the nucleophilicity of the $\sigma^3,\lambda^3$-P atom.[3] Compounds **3a** and **3b** were treated with one equivalent of bis(trimethylsilyl) peroxide, elemental sulfur, [W(CO)$_5$(thf)] and methyl trifluoromethanesulfonate to give phosphole oxides **4a** and **4b**, phosphole sulfides **5a** and **5b**, W complexes **7a** and **7b** and phospholium salts **8a** and **8b**, respectively (Scheme 2). Addition of one equivalent of selenium to **3b** afforded **6b**. These derivatives were isolated in high yields (Table 3) as air-stable solids, except for **4a** and **8a**, which bear 2-pyridyl substituents. Compound **4a** decomposes rapidly in THF or CH$_2$Cl$_2$ and was only observed by $^{31}$P NMR spectroscopy ($\delta = +42.4$). The slow decomposition of phospholium salt **8a** prevented satisfactory elemental analysis. The multinuclear NMR spectroscopic data of the isolated phospholes are typical[3] and support the proposed structures (Table 3). Complexes **7a**[9a] and **7b** were subjected to single-crystal X-ray diffraction studies (vide infra).

To evaluate the extent of the perturbation induced by these chemical modifications, the $^{13}$C NMR chemical shifts of the endocyclic phosphole carbon atoms of compounds **3a,b** were compared with those of their derivatives. The general trends are similar for both phospholes, and hence are discussed in detail only for bis(2-thienyl)phosphole **3b**. The chemical shifts of the C$_\alpha$ and C$_\beta$ atoms of the free and W(CO)$_5$-coordinated phosphole are comparable (**3b/7b**: $\Delta\delta < 1.1$), and this suggests that coordination of the phosphorus lone pair induces very little perturbation within the C skeleton of the phosphole ring. In comparison with the $\sigma^3$-phosphole **3b**, the C$_\beta$ atoms of the corresponding $\sigma^4$-phosphole oxide **4b**, sulfide **5b** and selenide **6b** are slightly deshielded ($0.7 > \Delta\delta > 1.7$), while the C$_\alpha$ atoms are considerably more shielded ($7.2 > \Delta\delta > 10.7$). This effect is even more pronounced for the cationic salt **8b**, the C$_\beta$ and the C$_\alpha$ signals of which are strongly deshielded (**3b/8b**, $\Delta\delta = 9.7$) and shielded (**3b/8b**, $\Delta\delta = 17.3$), respectively. These spectroscopic data, as a whole, suggest that gradual perturbation of the dienic moiety of the phosphole ring can be achieved by chemical modifications involving the P atom.

**Solid-state structures of free and W(CO)$_5$-coordinated 2,5-diheteroarylphospholes 3a and 3b**: The thienyl rings of the free[9b] and coordinated phosphole **3b** (Figure 3, Tables 1 and 2) exhibit a statistical disorder. This feature is typical for linear oligomers bearing terminal thiophene rings[2a, 10] and, as is usually observed for 2,5-bis(2-thienyl)heteroles,[2g,i] the two thienyl substituents have an *anti* arrangement with respect to the central phosphole ring in the prevailing conformation (80%). The free and W(CO)$_5$-coordinated forms of 2,5-bis(2-pyridyl)phosphole **3a**[9a] have the three heteroatoms in a mutual *syn,syn* arrangement. Theoretical calculations on the free phosphole (vide infra) show that this unexpected conformation is slightly more stable than the two other N,P,N arrangements (*syn,anti* and *anti,anti*).

The free and coordinated phospholes share some important structural features. The twist angles between two adjacent

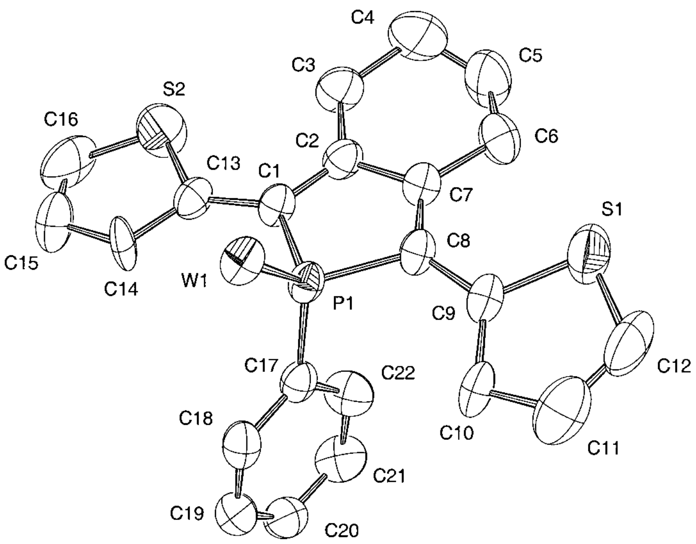

Figure 3. Molecular structure of complex **7b** in the solid state (50% probability thermal ellipsoids) with atom labelling for Table 1 (hydrogen atoms omitted for clarity).

rings are rather small [**3a**: 7.0(5), 25.6°(5); **3b**: 12.5(5), 16.7°(5); **7a**: 0.0(4), 11.3°(4); **7b**: 7.3(9), 13.4°(8)], and this allows extended π conjugation over the three heterocycles. For all compounds, the C–C bond lengths between the rings (C1–C13, C8–C4 1.436(6) – 1.467(8) Å; Table 1) and the endocyclic C2–C7 bond lengths (1.465(7) – 1.487(11) Å) are in the range expected for $C(sp^2)-C(sp^2)$ single bonds, while the endocyclic P–C bond lengths (1.817(4) – 1.821(8) Å) approach that of a P–C single bond (1.84 Å). Coordination of the phosphorus lone pair to the $W(CO)_5$ fragment has no noticeable influence on the CPC angles (Table 1), since the phosphorus atoms are strongly pyramidalised, as indicated by the sum of the C-P-C angles (**3a**, 299.3°; **3b**, 299.3°; **7a**, 299.0°; **7b**, 299.4°).

These solid-state data clearly show that the P lone pair of the $\sigma^3,\lambda^3$-phospholes **3a**,**b** is not conjugated with the endocyclic dienic framework and that, in line with the conclusion drawn from the $^{13}C$ NMR data, the coordination of the P atom by the $W(CO)_5$ fragment causes little perturbation in the phosphole ring. These data favour an extended delocalisation involving the dienic moiety of the phosphole rings and the two pyridyl or thienyl units.

**UV/Vis absorption and fluorescence spectra of 2,5-diheteroarylphospholes and derivatives**: It was of primary importance to study the influence of the hydrogen-bond donor ability (HBDA)[11] of the solvent on the photophysical properties of phospholes, since they all possess basic centres. Phosphole **3a**, bearing two pyridyl substituents, was selected for this study. The solvent has a noticeable influence on the absorption maximum, but the effect on the emission wavelength is negligible (Table 4). It is noteworthy that the bathochromic shift increases with increasing HBDA of the solvent. Therefore, the UV/Vis absorption and fluorescence spectra of all phospholes were recorded in the non-hydrogen-bonding solvent THF (Table 5).[11] All of the phospholes shown in Scheme 1 exhibit an absorption maximum in the visible region, attributed to π–π* transition of the extended conjugated system, and on excitation at $\lambda_{max}$, they emit in the visible region (Table 5).

Table 4. Influence of the solvent on the photophysical data for phosphole **3a**.[a]

| | $\lambda_{max}$ [nm] | $\log\varepsilon$ | $\lambda_{em}$ [nm] |
|---|---|---|---|
| THF | 390 | 4.02 | 463 |
| $CH_2Cl_2$ | 374 | 4.18 | 463 |
| $CHCl_3$ | 372 | 4.25 | 463 |
| EtOH | 364 | 4.19 | 466 |

[a] Absorption and emission maxima, ±3 nm.

An increase in the size of the fused carbocycle has almost no effect on $\lambda_{max}$ and $\lambda_{onset}$ (optical end absorption) in the UV/Vis spectra, but is accompanied by a blue shift in the emission spectra ($\lambda_{em}$: **3a**: 463 nm; **3d**: 480 nm). The $\lambda_{max}$ and $\lambda_{onset}$ values of *P*-alkylphosphole **3e** are about 20 nm to shorter wavelength than that of the corresponding *P*-phenylphosphole **3a**, but their $\lambda_{em}$ values are very similar (Table 5). Interestingly, the nature of the 2,5-substituents on the P-containing ring has a dramatic effect on the photophysical

Table 5. Photophysical[a] and electrochemical[b] data for 2,5-diarylphospholes and their derivatives.

| | $\lambda_{max}$ [nm][c] | $\lambda_{onset}$ [nm][c] | $\log\varepsilon$ | $\lambda_{em}$ [nm][c] | $\phi_f$[d] | $E_{pa}$ [V] | $E_{pc}$ [V] |
|---|---|---|---|---|---|---|---|
| **3a** | 390 | 448 | 4.02 | 463 | $1.1 \times 10^{-2}$ | +0.83 | −2.45 |
| **3b** | 412 | 468 | 3.93 | 501 | $5.0 \times 10^{-2}$ | +0.40 | – |
| **3c** | 354 | 430 | 4.20 | 466 | $14.3 \times 10^{-2}$ | +0.69 | −2.88 |
| **3d** | 395 | 442 | 3.96 | 480 | – | – | – |
| **3e** | 371 | 430 | 4.10 | 458 | – | +0.79 | −2.67 |
| **4b** | 434 | 500 | 3.97 | 556 | $0.69 \times 10^{-2}$[e] | +0.63 | −2.03 |
| **5a** | 364 | 444 | 3.94 | 470 | $0.004 \times 10^{-2}$ | +1.43 | −1.88 |
| **5b** | 432 | 496 | 3.98 | 548 | $4.6 \times 10^{-2}$[e] | +0.68 | −1.95 |
| **6b** | 423 | 503 | 4.09 | 547 | $0.12 \times 10^{-3}$[e] | +0.67 | −1.96 |
| **7a** | 373 | 443 | 4.01 | 465 | $0.002 \times 10^{-2}$ | +0.51 | −2.09 |
| **7b** | 408 | 475 | 4.04 | 506 | $1.3 \times 10^{-2}$[e] | +0.70 | −2.20 |
| **8a** | 394 | 458 | 3.98 | 510 | $6.8 \times 10^{-2}$ | >+1.8 | −1.29 |
| **8b** | 442 | 528 | 3.92 | 593 | $0.8 \times 10^{-2}$[e] | +0.92 | −1.66 |

[a] Measured in THF. [b] All potentials were obtained during cyclic voltammetric investigations in 0.2 M $Bu_4NPF_6$ in $CH_2Cl_2$. Platinum electrode diameter 1 mm, sweep rate: 200 mV s$^{-1}$. All reported potentials are referenced to the reversible formal potential of the ferrocene/ferrocenium couple. [c] Absorption and emission maxima, ±3 nm; $\lambda_{onset}$, ±5 nm. [d] Fluorescence quantum yields determined relative to quinine sulfate unless otherwise stated, ±15%. [e] Relative to fluorescein, ±15%.

properties of related phospholes **3a–c**. A noticeable red shift in the absorption spectra is observed on replacing the phenyl groups either by 2-pyridyl ($\Delta\lambda_{max} = 36$ nm) or 2-thienyl groups ($\Delta\lambda_{max} = 58$ nm); this effect is less pronounced for $\lambda_{onset}$ (Table 5). A blue-green emission is observed for diphenyl- and bis(2-pyridyl)phospholes **3a** and **3c** (463–466 nm), and the emission of bis(2-thienyl)phosphole **3b** is red-shifted ($\Delta\lambda_{em} = 35$ nm). The Stokes shift of **3c** (112 nm) is considerably larger than those of heteroaryl-substituted **3a** (73 nm) and **3b** (89 nm). The quantum yields also depend on the 2,5-substitution pattern, the highest ($14.3 \times 10^{-2}$) being observed for **3c** (Table 5).

Further variations of the photophysical properties of phospholes can be achieved by chemical modifications involving the P atom. The same chemical transformation (coordination, oxidation by chalcogens, alkylation) has different, and sometimes opposite, effects within the pyridyl- and thienylphosphole series. Coordination of the P atom to a $W(CO)_5$ fragment has a relatively modest impact. Complex **7a** exhibits a maximum absorption at a shorter wavelength than the free phosphole **3a** and a comparable emission spectrum (**3a**/**7a**, $\Delta\lambda_{max} = 17$ nm, $\Delta\lambda_{em} = 2$ nm), whereas free and coordinated **3b** exhibit very similar photophysical data (Table 5). Oxidation of the P atom to give $\sigma^4$ derivatives has a more pronounced effect. Comparison of the absorption spectra of $\sigma^3$-phosphole **3a** and $\sigma^4$-thiooxophosphole **5a** reveals a blue shift in $\lambda_{max}$ (**5a**/**3a**, $\Delta\lambda_{max} = 26$ nm), but similar $\lambda_{onset}$ (Table 5). In contrast, a red shift was observed for the corresponding dithienyl derivatives (**5b**/**3b**, $\Delta\lambda_{max} = 20$ nm, $\Delta\lambda_{onset} = 28$ nm). Both series exhibit bathochromic shifts in the emission maxima on oxidation of the P atom with chalcogens. This effect is much weaker for the pyridyl- (**3a**/**5a**, $\Delta\lambda_{em} = 7$ nm) than for the thienyl-substituted phospholes (**3b**/**4b–6b**, $\Delta\lambda_{em} = 46–55$ nm). Note that the Stokes shifts are almost the same in both series (106–116 nm). The most important perturbation of the photophysical properties of phospholes **3a**,**b** was achieved by alkylation to give phospholium salts **8a**,**b**. Although the absorption maxima and optical end absorption of 2,5-dipyridyl derivatives **3a** and **8a** are similar (Table 5), the $\lambda_{em}$ of **8a** is considerably red-shifted relative to that of **3a** (**8a**/**3a**, $\Delta\lambda_{em} = 47$ nm). In other words, the Stokes shift of **8a** (116 nm) is far larger than that of **3a** (73 nm). The effects are even more pronounced for dithienylphospholes **3b** and **8b**: large red-shifts are observed in both the absorption (**8b**/**3b**, $\Delta\lambda_{max} = 30$ nm, $\Delta\lambda_{onset} = 60$ nm) and the emission (**8b**/**3b**, $\Delta\lambda_{em} = 92$ nm) spectra, and the increase in the Stokes shift is 61 nm (Table 5).

The $\sigma^4$-phospholes generally exhibit lower quantum yields than the corresponding $\sigma^3$-phospholes (Table 5), with the sole exception of the phospholium salt **8a** (**3a**, $1.1 \times 10^{-2}$; **8a**, $6.8 \times 10^{-2}$).

**Electrochemical behaviour of 2,5-diheteroarylphospholes and derivatives**: Cyclic voltammetry (CV) at 200 mV s$^{-1}$ revealed that the redox processes observed for all the $\sigma^3$- and $\sigma^4$-phospholes are irreversible. As is usually found for short oligothiophenes,[1d, 12] several oxidation steps are recorded for the neutral derivatives (vide infra, Table 8); the first anodic ($E_{pa}$) and cathodic peak ($E_{pc}$) potentials are given in Table 5. The reduction wave of **3b** ($E_{pc} < -2.10$ V) does not have the classical shape expected for an irreversible electrochemical wave and is suggestive of a rapid electrochemical/chemical process. As a consequence, the $E_{pc}$ of compound **3b** can not be unambiguously assigned. The redox potentials of $\sigma^3,\lambda^3$-phospholes **3a–c** are related to the electronic properties of the 2,5-substituents. For example, **3b** containing electron-rich thienyl substituents is more easily oxidised than **3a** possessing electron-poor pyridyl substituents, whereas 2,5-diphenylphosphole **3c** exhibits an intermediate potential (Table 5).

$\sigma^4$-Phospholes have lower reduction and higher oxidation potentials than the corresponding $\sigma^3$-phospholes (Figure 4). For example, **3b** has an $E_{pa}$ at $+0.40$ V and $E_{pc}$ at a potential less cathodic than $-2.10$ V, while for the phospholium salt **8b** these peak potentials are at $+0.92$ V and $-1.66$ V, respectively. Compounds **4b**, **5b** and **6b** show intermediate $E_{pa}$ ($+0.63–0.68$ V) and $E_{pc}$ ($-2.03$ to $-1.95$ V) values and, in spite of the different electronegativities of the chalcogen atoms, they exhibit similar electrochemical behaviour. The same trend is observed for pyridyl-substituted phospholes **3a**, **5a** and **8a** (Figure 4). Note that the data for the complexes **7a** and **7b** should be treated with some caution, since the redox processes could involve the transition metal centre.[13]

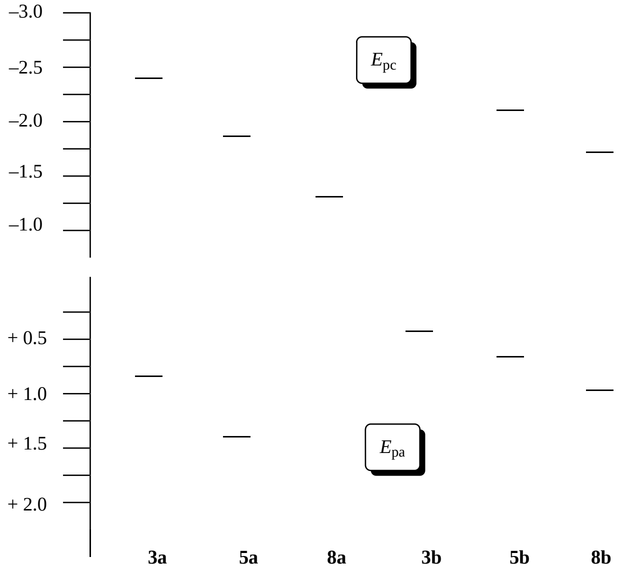

Figure 4. First oxidation ($E_{pa}$) and reduction ($E_{pc}$) peak potentials for 2,5-diarylphospholes **3a**,**b** and their $\sigma^4$ derivatives **5a**,**b** and **8a**,**b**.

**Theoretical calculations on 2,5-diarylphospholes and their derivatives**: The three heterocycles of the parent 2,5-diheteroarylphospholes **3a′** and **3b′** (Table 6) are nearly coplanar. As a consequence, the nitrogen or sulfur atoms can be in a *syn* or an *anti* position with respect to the phosphorus atom, so that three isomers (*syn*,*syn*, *syn*,*anti* and *anti*,*anti*) are possible. For both phospholes, all of these structures are minima on the potential energy surface. The *syn*,*syn* arrangement is the lowest energy structure for 2,5-dipyridylphosphole (**3a′**). However, this isomer is only 1.0 and 4.8 kJ mol$^{-1}$ more stable than the *syn*,*anti* and *anti*,*anti* isomers, respectively. In

Table 6. Selected B3LYP/6-31 + G* bond lengths [in Å], LUMO and HOMO energies [HF/6-31 + G*//B3LYP/6-31 + G*, in eV], and total energies [B3LYP/6-31 + G*, in au] of the parent 2,5-diarylphospholes.

| 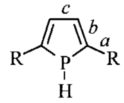 |  | *a* | *b* | *c* | LUMO | HOMO | Total energies |
|---|---|---|---|---|---|---|---|
| **3a′** | R = 2-pyridyl | 1.463 | 1.372 | 1.441 | 0.97 | – 7.49 | – 990.96705 |
| **3b′** | R = 2-thienyl | 1.449 | 1.371 | 1.442 | 0.96 | – 7.17 | – 1600.39289 |
| **3c′** | R = phenyl | 1.467 | 1.367 | 1.451 | 1.24 | – 7.36 | – 958.88540 |

contrast, for 2,5-dithienylphosphole (**3b′**), the *anti*,*anti* arrangement is the lowest energy structure, again with a rather small energy difference of 8.1 kJ mol$^{-1}$. The energies of the transition structures for rotation about the inter-ring C–C bonds are comparable for pyridyl- and thienyl-substituted phospholes, and barriers to rotation are low (12 – 16 kJ mol$^{-1}$).

The inter-ring C–C distances should be dependent on the degree of conjugation of the $\pi$ system over the three rings. A decrease in the inter-ring C–C bond length is observed on replacing the phenyl by a thienyl substituent (Table 6), and this suggests that the most effective conjugation is attained in 2,5-dithienylphosphole (**3b′**). This result prompted us to compare **3b′** with 2,5-dithienylheterocyclopentadienes **E** (Table 7), which contain central units with different electronic characters. An aromatic electron-rich thiophene[2f, 5d] and a nonaromatic electron-deficient silole were selected.[2j, 5d] Some important calculated structural data and HOMO/LUMO energies for these compounds are presented in Table 7, together with the LUMO energies of the parent central heterocyclopentadiene. The difference in parameters *b* and *c* (bond length alternation) gives an estimation of the delocalisation within the central ring of 2,5-dithienylheterocyclopentadienes **E**. As expected from their aromatic character, this endocyclic conjugation is higher for thiophene than for phosphole and silole rings, as concluded from the change in the C–C bond length alternation (Table 7). Interestingly, the LUMO level of the phosphole is close to that of the silole, which is known as a highly electron-deficient heterocycle. The inter-ring C–C distances for phosphole- and silole-containing oligomers are comparable, and slightly shorter ($\Delta a = 0.005$ Å) than that observed for terthiophene. This structural change, which indicates increased delocalisation of the $\pi$ system over the three rings, is related to the electronic properties of the central heterocyclopentadiene unit, that is, a weak aromatic character and stabilisation of the LUMO favour extended conjugation. The LUMO and HOMO of 2,5-dithienylheterocyclopentadienes are $\pi$ orbitals and are stabilised and destabilised, respectively, in the thiophene, phosphole, silole series (Figure 5). In other words, the HOMO – LUMO gap gradually decreases on replacing the central thiophene ring by a phosphole and a silole moiety. Although the differences in the bond lengths are rather small, these trends are also reproduced at the B3LYP/6-21(G*) level of theory.

Table 7. LUMO energies [HF/6-31 + G*//B3LYP/6-31 + G*, in eV] of the parent heterocycles and selected B3LYP/6-31 + G* bond lengths (in Å), LUMO and HOMO energies [HF/6-31 + G*//B3LYP/6-31 + G*, in eV], and total energies [B3LYP/6-31 + G*, in au] of dithienyl substituted heterocyclopentadienes **E**.

|  | 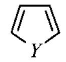 | 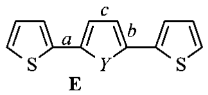<br>**E** |  |  |  |  |  |
|---|---|---|---|---|---|---|---|
| Y | LUMO | *a* | *b* | *c* | LUMO | HOMO | Total energies |
| S | 2.14 | 1.453 | 1.381 | 1.419 | 1.29 | – 7.37 | – 1656.64883 |
| PH | 1.50 | 1.449 | 1.371 | 1.442 | 0.96 | – 7.17 | – 1600.39289 |
| SiH$_2$ | 1.39 | 1.448 | 1.369 | 1.460 | 0.77 | – 7.06 | – 1547.87854 |
| PF | 1.30 | 1.447 | 1.367 | 1.451 | 0.43 | – 7.24 | – 1699.65674 |
| P(O)H | 1.15 | 1.445 | 1.363 | 1.460 | 0.37 | – 7.49 | – 1675.62613 |
| P(S)H | 1.04 | 1.447 | 1.363 | 1.455 | 0.33 | – 7.57 | – 1998.59164 |
| P(O)F | 0.86 | 1.443 | 1.362 | 1.465 | 0.19 | – 7.62 | – 1774.91782 |

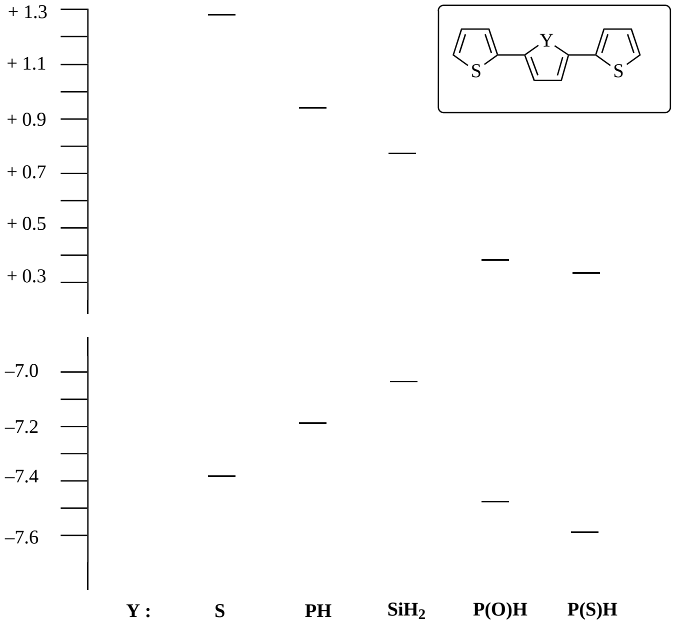

Figure 5. HF/6-31 + G* HOMOs and LUMOs of 2,5-bis(2-thienyl)heterocyclopentadienes **E**.

The impact of the nature of the substituent and of chemical modifications of the $\sigma^3,\lambda^3$-phosphorus atom were investigated for the parent 2,5-bis(2-thienyl)phosphole **3b′**. Replacing the hydrogen atom on P by an electronegative fluorine atom slightly shortens the inter-ring distance ($\Delta a = 0.002$ Å) and increases the difference in bond lengths of the phosphole carbon framework (Table 7). The same trends are observed on oxidation of the phosphorus atom to give nonaromatic $\sigma^4$-phosphole oxides or sulfides (Table 7). The calculated structural data of oxo- and thiooxodithienylphospholes are very similar, and their LUMOs and HOMOs are $\pi$ orbitals that are mainly localised on the carbon framework (Figure 6). Importantly, $\sigma^4$-oxodithienylphospholes have stabilised LUMO and HOMO levels and smaller HOMO – LUMO gaps relative to the corresponding $\sigma^3$-phosphole **3b′** (Figure 5).

**Anodic oxidation of 2,5-bis(2-thienyl)phosphole 3b and derivatives**: 2,5-Bis(2-thienyl)phosphole derivatives were subjected to electro-oxidation processes to prepare $\pi$-conjugated oligomers or polymers.[1c, 12a, b] These experiments were conducted in CH$_2$Cl$_2$ containing 0.2 M Bu$_4$NPF$_6$ at a scan rate of 100 mV s$^{-1}$ and revealed anodic behaviours that were

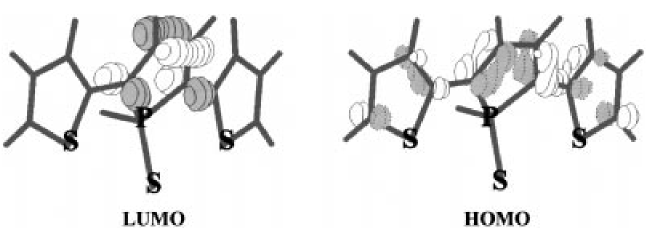

Figure 6. HF/6-31 + G* HOMO and LUMO of 2,5-bis(2-thienyl)thiooxophosphole (**3b′**).

related to the nature of the phosphorus moiety. σ$^4$-Phosphole derivatives **4b** and **5b** exhibited two irreversible oxidation processes with formation of films on the Pt working electrode on reaching the second oxidation potential $E_{pa2}$ (Table 8). The efficiency of the polymerisation process increased until the optimum polymerisation potential $E_{op}$, determined by chronoamperometry, was reached (Table 8). These two compounds exhibit similar behaviour, and a typical cyclic voltamogram (CV) obtained for **5b** is shown in Figure 7a. The initial scan is characterised by a relatively sharp onset of the first monomer oxidation peak, followed by a reductive process on the return cycle. In a subsequent potential sweep, an oxidation wave appeared at a less positive potential than that for monomer oxidation. Repeated cycling resulted in a regular increase in the oxidation and reduction peak currents of this new reversible system; this indicates the deposition of insoluble electroactive material on the platinum surface. The CVs of σ$^4$-phospholium salt **8b** showed only one oxidation step at 0.92 V, a value close to $E_{pa2}$ of **4b** and **5b**, and an electroactive film formed on recurrent cycling between 0 and 1.20 V (Figure 7b). σ$^3$-Phosphole **3b** exhibited a quite peculiar anodic behaviour. During recurrent CVs an electroactive film formed, albeit in low yield (Figure 7c). The first oxidation step observed in the initial sweep at 0.40 V is shifted to the threshold potential of the formed polymer (0.63 V) upon repeated cycles (Figure 7c), due to the insulating behaviour of the undoped polymer between 0 and 0.5 V (Figure 8c). It is noteworthy that the formation of electroactive films depends dramatically on the experimental conditions. For example, with for a solution of monomers **3b** and **8b** in $CH_3CN$ with $LiClO_4$ as electrolyte salt, no film was formed.[9b]

Table 8. Second oxidation potentials and optimum polymerisation potential of monomers **3b**–**5b** and **8b**. *p*-Doping and *n*-doping potential ranges [V] and photophysical data of the corresponding dedoped polymers.[a]

| | $E_{pa2}$ | $E_{op}$[b] | | *p*-doping[c] | *n*-doping[c] | $\lambda_{max}$[e] | $\lambda_{onset}$[e] |
|---|---|---|---|---|---|---|---|
| **3b** | 1.00 | 1.00 | poly-**3b** | 0.50 → 0.85 | −0.60 → −1.00 | 463–567 | 724 |
| **4b** | 0.95 | 1.10 | poly-**4b** | 0.25 → 0.60 | −1.40 → −1.92 | 568 | 780 |
| **5b** | 0.90 | 1.15 | poly-**5b** | 0.30 → 0.65 | −1.80 → −2.42 | 529 | 750 |
| **8b** | – | 1.20 | poly-**8b** | 0.40 → 0.70 | −0.60[d] | 627 | 905 |

[a] All potentials were obtained during cyclic voltammetric investigations in 0.2 M $Bu_4NPF_6$ in $CH_2Cl_2$: $10^{-2}$ M solution of monomers or in 0.1 M $Bu_4NPF_6$ in $CH_3CN$ free of monomer for the polymer response. Platinum electrode diameter 1 mm, sweep rate: 100 mV s$^{-1}$. [b] $E_{op}$ were obtained by chronoamperometric investigations. [c] Potentials range where the *p*- and *n*-doping processes are reversible. Potentials referred to the ferrocene/ferrocenium. [d] Threshold reduction potential of the irreversible process. [e] ± 5 nm.

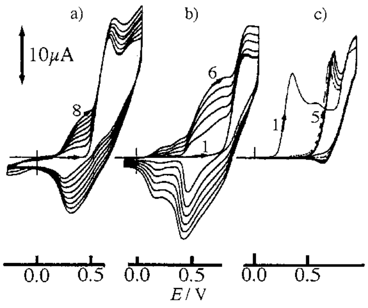

Figure 7. Multiple-scan voltammogram of $10^{-2}$ M solutions of a) **5b**, b) **8b** and c) **3b** in 0.2 M $Bu_4NPF_6$ in $CH_2Cl_2$ (scan rate: 100 mV s$^{-1}$). Working electrode: platinum disc ($d$ = 1 mm). Potentials relative to Fc/Fc$^+$.

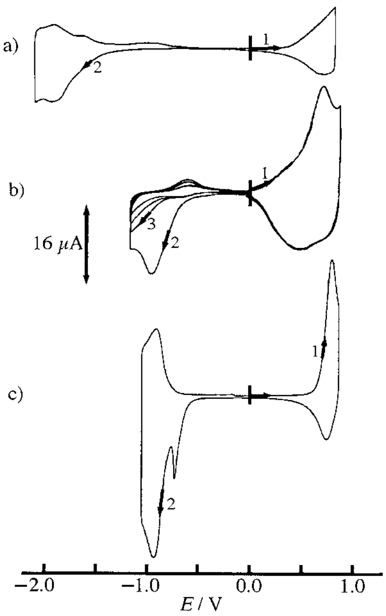

Figure 8. Cyclic voltammograms of electropolymerised a) poly-**5b**, b) poly-**8b** and c) poly-**3b** recorded in 0.2 M $Bu_4NPF_6$ in $CH_3CN$ (scan rate, 100 mV s$^{-1}$). Working electrode: platinum disc ($d$ = 1 mm) modified by anodic oxidation of $10^{-2}$ M solutions of **5b** (at $E$ = 1.15 V, $Q_t$ = 7.5 × $10^{-4}$ C), **8b** (5 sweeps between 0.0 and 0.88 V) and **3b** (at $E$ = 1.00 V, $Q_t$ = 5.0 × $10^{-4}$ C) in 0.2 M $Bu_4NPF_6$ in $CH_2Cl_2$. Potentials relative to Fc/Fc$^+$.

All of the polymers can also be obtained by oxidation at $E_{op}$, as determined by chronoamperometry (Table 8). The films are insoluble in all common solvents ($CH_2Cl_2$, THF, DMF, acetone, acetonitrile, MeOH). The modified electrodes were rinsed with $CH_2Cl_2$ and studied by CV in monomer-free solutions of $CH_3CN$ containing 0.1 M $Bu_4NPF_6$ at a scan rate of 100 mV s$^{-1}$. The polymers prepared with neutral phospholes **3b**, **4b** and **5b** exhibited *p*- and *n*-doping processes with good reversibility (> 70 %) (Figure 8a,c). Poly-**8b** also exhibited reversible *p* doping, but its electroactivity dramatically decreased upon reduction (Figure 8b). The doping processes are observed in potential ranges that depend on the nature of the phosphole monomer (Table 8). It is noteworthy that these processes appeared at lower potentials than those of the corresponding 2,5-dithienylphospholes, and this suggests that the electroactive materials formed on the electrode have longer conjugation pathways and smaller band gaps than the monomers.

**UV/Vis absorption spectra of poly[(2,5-dithieny)phospholes]**: Thin-film absorption spectra were recorded to probe the electronic nature of the polymers. The material was deposited at $E_{op}$ on discs of mirror-polished platinum and then dedoped at 0.0 V. Poly-**3b** exhibits two large bands with unresolved maxima at about 463 and 567 nm (Figure 9c) with a $\lambda_{onset}$ at 734 nm. The other materials exhibited only one broad absorption band in the visible region (Figure 9a,b, Table 8). Two important features emerge: 1) the optical properties of the material are sensitive to the nature of the monomer, and 2) the $\lambda_{onset}$ are considerably red-shifted relative to those of the corresponding monomers ($\Delta\lambda_{onset}$: **3b**: 162 nm; **4b**: 280 nm; **5b**: 254 nm; **8b**: 385 nm).

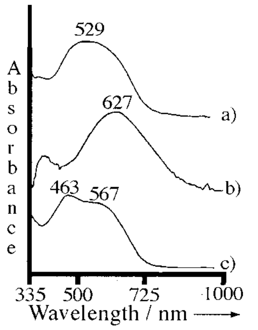

Figure 9. Electronic absorption spectra in $CH_2Cl_2$ on mirror-polished platinum discs modified with a) poly-**5b**, b) poly-**8b** and c) poly-**3b** after dedoping at 0.0 V. Deposits were prepared by anodic oxidation of $10^{-2}$ M solutions of **5b** (at $E = 1.15$ V), **8b** (at $E = 1.20$ V) and **3b** (at $E = 1.00$ V) in 0.2 M $Bu_4NPF_6$ in $CH_2Cl_2$. Absorbance: arbitrary units.

**Synthesis and optical properties of oligomer 11**: Mixed thiophene–thiooxophosphole oligomer **11** (23% yield) was prepared according to the general strategy of Tilley et al. for the synthesis of phenylene–thiophene 1-oxide oligomers (Scheme 3).[2h] Compound **11** was purified by column chromatography on basic alumina. It exhibits a singlet at $\delta = +52.6$ in the $^{31}P$ NMR spectrum, and was characterised by multinuclear NMR spectroscopy and high-resolution mass spectrometry. This oligomer is soluble in polar solvents ($CH_2Cl_2$, THF, MeOH) and exhibits an absorption maximum in the UV/Vis spectrum at 512 nm with a $\lambda_{onset}$ at 600 nm.

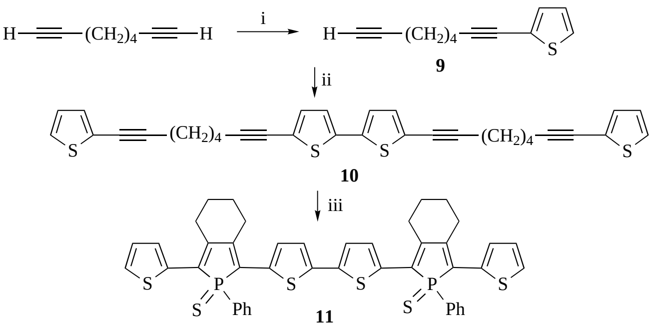

Scheme 3. Synthesis of mixed thiophene–thiooxophosphole derivative **11**. i) 2-Iodothiophene, 2% $[PdCl_2(PPh_3)_2]$, 2% CuI, $Et_3N$, RT, 7 h; ii) 5,5′-dibromo-2,2′-bithiophene, 2% $[PdCl_2(PPh_3)_2]$, 2% CuI, $Et_3N$, RT, 48 h; iii) $[Cp_2ZrCl_2]$ (2 equiv), *n*BuLi (4.1 equiv), THF, −78 °C to RT, 12 h; $PhPBr_2$ (2 equiv), THF, −78 °C, then 24 h, 40 °C; 1/4 $S_8$, THF, RT, 36 h.

## Discussion

Pyridyl- and thienyl-substituted $\sigma^3,\lambda^3$-phospholes **3a,b** are readily available on a gramme scale by the Fagan–Nugent method (Scheme 1) and are easy to handle provided they have a phenyl substituent on the P atom. $\sigma^4$-Phosphole derivatives are even more stable, with the exception of pyridyl-substituted oxophosphole **4a** and phospholium salt **8a**.

Among the various structural variations aimed at tuning the properties of phosphole-based π-conjugated oligomers (Figure 1, compound **D**), the nature of the 2,5-substituents and chemical modification of the P atom appear to be crucial. The redox potentials of phosphole-containing oligomers dramatically depend on the nature of the 2,5-substituents (Figure 4), which allow their HOMO and LUMO levels to be controlled over a wide range. The theoretical calculations, based on the analysis of the inter-ring distances *a* (Table 6), predict that the delocalisation of the π system increases on replacing a phenyl by a pyridyl group and reaches a maximum with the thienyl substituents. This behaviour is in full agreement with the measured longest-wavelength absorption maximum and the optical end absorption (the optical "HOMO–LUMO" gap in solution; Table 5)[1i]. Although care must be taken when comparing photophysical data from different sources, it is interesting to compare the general influence of the 2,5-substitution pattern for siloles[2j] and phospholes, two classes of nonaromatic heterocycles. The $\lambda_{max}$ of 2,5-diarylsiloles increases in the series of 2,5-substituents: phenyl (359 nm), 2-pyridyl (370 nm), 2-thienyl (418 nm).[2j] In contrast, the phenyl- and 2-pyridylsiloles emit at the same wavelength (467–468 nm), whereas the 2-thienylsilole shows a 47 nm red shift in emission.[2j] It is remarkable that these general trends are similar to those of phospholes (Table 5). Furthermore, note that phosphole **3b** has a much longer $\lambda_{max}$ (412 nm) than related bis(2-thienyl)heterocyclopentadienes of type **E** (see Table 7) containing electron-rich aromatic rings with central Group 15 or Group 16 atoms ($Y = NCH_3$, 322 nm;[2o, 14] O, 366 nm;[2p] S, 356 nm[2i]). As outlined by theoretical calculations (Table 7), this is probably due to the fact that siloles and phospholes share some important electronic properties: low-lying LUMOs and nonaromatic character. This analogy is promising, since 2,5-diarylsiloles have found applications as electron-transporting materials in organic light-emitting diodes.[2j,m, 16a] Furthermore, in contrast to other heterocyclopentadienes (e.g., siloles, pyrroles), phospholes have a reactive heteroatom that allows a family of π-conjugated systems to be prepared from a single P-containing chromophore. Oxidation of the P atom makes the phosphole ring an electron-poor heterocycle. As suggested by the multinuclear NMR data, the electron deficiency of $\sigma^4,\lambda^4$-phosphole derivatives can be gradually modulated by preparing neutral compounds with polarised $P^{\delta+}{=}Y^{\delta-}$ (Y = O, S, Se) bonds or phospholium salts. Thienyl- and pyridyl-substituted phosphole derivatives will be discussed in separate sections, since the effect of the chemical modifications are not the same in both series.

An important conclusion of the theoretical calculations was that oxo- and thiooxodithienylphospholes should exhibit very different electronic properties (stabilised HOMO and LUMO, smaller HOMO–LUMO gaps) than the corresponding $\sigma^3$-phosphole (Figure 5). These results are indeed in line with the experimental data: red-shifted absorptions, optical end absorption and emission maxima were observed on oxidation of the P atom of **3b** with elemental sulfur, selenium or peroxides (Table 5), along with stabilisation of the LUMO and HOMO (Figure 4). Note that these trends are amplified for the phospholium salt **8b**, which has the highest $\lambda_{max}$ and $\lambda_{onset}$ (Table 5), along with the lowest $E_{pa}$ and $E_{pc}$ (Figure 4). These features of the thienyl series are in line with the general trend that maximum π conjugation is obtained with alternating electron-rich and electron-poor heterocycles.[2] The tuning of the emission wavelengths by chemical modification of the P atom is particularly noteworthy. This family of chromophores covers a range of 92 nm in the emission spectra, with Stokes shifts gradually increasing in the series: $\sigma^3$-phosphole **3b** (89 nm), $\sigma^4$-phosphole **5b** (116 nm), phospholium salt **8b** (151 nm).

The properties of pyridyl-substituted phospholes can also be tuned by chemical modification of the P atom. As observed in the thienyl series, the HOMO and LUMO are gradually stabilised on increasing the positive charge on the P-atom (Figure 4). The pyridyl-substituted phospholes have lower lying HOMOs and LUMOs than the corresponding compounds with thienyl substituents. Importantly, **5a** has a low reduction potential, comparable to those observed for highly electron deficient systems (e.g., 2,5-dithiazolylsiloles[2j] and poly(quinoxaline-2,6-diyl)[15]). This property is particularly important for the development of new electron-transporting (ET) materials suitable for the preparation of organic electroluminescent devices, since an efficient ET material should possess a high electron affinity to decrease the energy barrier for electron injection.[16] The optical properties of pyridyl-substituted phospholes are less strongly influenced by chemical modification of the P atom. Oxidation with sulfur or coordination to a $W(CO)_5$ fragment induces a significant blue shift in $\lambda_{max}$, a trend which is not observed upon alkylation of the P atom. Note that $\lambda_{onset}$ remains almost unchanged (Table 5). As observed in the thienyl series, the Stokes shift of the phospholium salt **8a** (116 nm) is far larger than that of the $\sigma^3$-phosphole **3a** (73 nm).

Model compounds **3a–c** revealed important structure–property relationships of phosphole-containing π-conjugated systems. Mixed phosphole–thiophene derivatives appeared to be particularly interesting, since they have small optical HOMO–LUMO gaps, and their optical and electrochemical properties vary over a wide range depending on the nature of the phosphorus moiety. These properties prompted us to investigate the preparation of polymers incorporating 2,5-bis(2-thienyl)phosphole units. One of the most versatile routes toward π-conjugated polymers is oxidative electropolymerisation of thienyl monomers.[1d, 12] Indeed, insoluble materials were obtained by this method for 2,5-dithienylphospholes with $\sigma^3$-P and neutral or cationic $\sigma^4$-P atoms. It is difficult to establish the degree of polymerisation and the intimate structure of these materials due to their insolubility, which prevents analysis by gel permeation chromatography and standard spectroscopic studies. It is well established that the major process during the electropolymerisation of oligothiophenes is an $\alpha,\alpha'$ coupling.[1d, 12a,b] Hence, we prepared model compound **11** by the Fagan–Nugent route (Scheme 3), which formally involves $\alpha,\alpha'$ coupling of 2,5-bis(2-thienyl)-thiooxophosphole **5b**. The comparison of the properties of the monomer **5b**, "dimer" **11** and poly-**5b** revealed some important features. First, unlike poly-**5b**, **11** is soluble in conventional polar solvents. Second, a bathochromic shifts in $\lambda_{onset}$ are observed in the series **5b** (496 nm), **11** (600 nm) and poly-**5b** (754 nm). The insolubility of poly-**5b**, along with the gradual narrowing of the optical band gap upon chain extension, suggests that the material obtained by electropolymerisation of **5b** consist of long oligomers with 2,5-dithienylphosphole as the repeating unit. This assumption can probably be extended to all materials derived from 2,5-dithienylphosphole monomers, since 1) all the films obtained on the working electrode exhibit considerably longer $\lambda_{max}$ and $\lambda_{onset}$ than those of the corresponding monomers (Tables 5 and 8), and 2) as is observed for the P-containing monomers, the electrochemical and photophysical data of these materials depend on the nature of the phosphorus moiety (Table 8). It is likely that the phosphorus atoms of the as-synthesised film of poly-**3b** are protonated, at least partially, since the electropolymerisation process produces protons.

The electro-oxidation of 2,5-dithienylphospholes produces materials with small optical band gaps, and poly-**8b** has a particularly high $\lambda_{onset}$ (Table 8). The polymers derived from neutral phospholes **3b**, **4b** and **5b** exhibit reversible *p*- and *n*-doping at rather low potentials (Table 8). These interesting properties are worthy of further investigation, and in situ spectroelectrochemical studies of the *p*-doping processes of these polymers are underway.

## Conclusion

π-Conjugated oligomers or polymers based on heterocyclopentadienes incorporating heavy heteroatoms in the main chain are still rare,[2i–n, q, 4] and this study showed that phosphole rings are valuable building blocks for the preparation of π-conjugated systems. The optical and electrochemical properties of 2,5-diheteroarylphospholes can be easily tuned over a wide range by tailoring the 2,5-substituents or by performing simple chemical modifications involving the nucleophilic P atom. These small oligomers allowed structure–property relationships to be established on the basis of experimental and theoretical data. 2,5-Dithienylphosphole derivatives proved to be valuable precursors to polymers with different optical and electronic properties by electro-oxidation. The good stability of the phosphole ring, along with its specific electronic properties, which profoundly differ from those of other Group 15 and 16 heterocyclopentadienes, opens new perspectives in the chemistry of π-conjugated systems incorporating heavy heteroatoms.[17]

## Experimental Section

**General**: All experiments were performed under dry argon by using standard Schlenk techniques. Solvents were freshly distilled under argon from sodium/benzophenone (tetrahydrofuran, diethyl ether) or phosphorus pentoxide (pentane, dichloromethane, acetonitrile). Triethylamine was freshly distilled under argon from potassium hydroxide. 2-Bromopyridine, 2-iodothiophene, octa-1,7-diyne, hepta-1,6-diyne, $[Cp_2ZrCl_2]$, CuI, *n*-BuLi, *i*$PrPCl_2$ and $PhPCl_2$ were obtained from Aldrich and were used as received. Melting points are uncorrected. $^1H$, $^{13}C$ and $^{31}P$ NMR spectra were recorded on Bruker AM300, DPX200 or ARX400 spectrometers. $^1H$ and $^{13}C$ NMR chemical shifts are reported relative to $Me_4Si$ as external standard. $^{31}P$ NMR downfield chemical shifts are expressed with a positive sign relative to external 85% $H_3PO_4$. Assignments of carbon atoms was based on HMBC and HMQC experiments. Melting and decomposition points were determined with a differential scanning calorimeter (TA-instruments DSC 2010) and a thermogravimetric analyser (TA-instruments TGA 2050), respectively. Transmittance FTIR spectra were obtained on a IFS-28 Bruker spectrometer (400–4000 $cm^{-1}$). High-resolution mass spectra were obtained on a Varian MAT311 or ZabSpec TOF Micromass at CRMPO, University of Rennes. Elemental analyses were performed by the "Centre de Microanalyse du CNRS" at Vernaison, France. Conventional glassware was used.

**Starting materials**: The starting materials were prepared according to literature procedures: 1,8-bis(2-thienyl)octa-1,7-diyne (**1b**),[18a] 1,8-diphenylhepta-1,7-diyne (**1c**),[18a] 1,7-bis(2-pyridyl)hepta-1,6-diyne (**1d**),[18a] $PhPBr_2$,[18b] bis(trimethylsilyl)peroxide,[18c] 5,5′-dibromo-2,2′-bithiophene.[18d]

**Determination of optical data**: UV/Vis spectra were recorded at room temperature on a UVIKON 942 spectrophotometer, and luminescence spectra were recorded in freshly distilled solvents at room temperature with a PTI spectrofluorimeter (PTI-814 PDS, MD 5020, LPS 220B) using a xenon lamp. Quantum yields were calculated relative to quinine sulfate ($\Phi = 0.546$ in 1N $H_2SO_4$)[19] or fluorescein ($\Phi = 0.90$ in 1N NaOH)[19]. For the UV/Vis spectra of poly(2,5-dithienylphosphole) derivatives, the materials were deposited on discs of mirror-polished platinum at $E_{op}$ and then dedoped at 0.0 V. The spectra were recorded on a Guided Wave Model 150 spectrophotometer with optical fibers.[20]

**Theoretical calculations**: Calculations were performed with the Gaussian 98[21] suite of programs at the B3LYP/6-31 + G* level of theory. The geometries were fully optimized without any symmetry constraints. At the optimized geometries, second derivatives were calculated, and positive eigenvectors of the Hessian matrix proved that true minima had been obtained. Transition structures for the rotation about the inter-ring C–C bonds were characterised by a single negative eigenvalue of the Hessian matrix. Orbital energies were obtained on the B3LYP/6-31 + G* optimized geometries at the HF/6-31 + G* level of theory. The MO diagrams were generated with MOLDEN 3.6, G. Schaftenaar CMBI University, Nijmegen (The Netherlands)

**Cyclic voltammetry measurements and electropolymerisation experiments**: Electrochemical measurements were performed in dichloromethane (Puran No. 02910E21) from SDS with less than 100 ppm of water. Tetra-*N*-butylammonium hexafluorophosphate from Fluka was used as received. Aluminum oxide from Woëlm (Super I) was heated at 300 °C under vacuum for 24 h and used at once under argon pressure. All the electrochemical investigations were carried out in a conventional three-compartment cell: in all cases the anode, the cathode and the reference electrode were separated by a glass frit. The working electrode was a polished platinum disc, and the counterelectrode was a glassy carbon rod. The reference electrode consisted of a silver wire in contact with 0.1M $AgNO_3$. Ferrocene was added to the electrolytic solution at the end of a series of experiments. The ferrocene/ferrocenium ($Fc/Fc^+$) couple served as an internal standard and all reported potentials are referenced to its reversible formal potential. All experiments were carried out under an argon atmosphere, and neutral alumina was added to the supporting electrolyte in the anodic compartment of the cell to remove excess moisture. The three-electrode cell was connected to an EG&G PAR model 173 potentiostat, monitored with a PAR model 179 signal generator and a digital coulometer PAR model 179. The cyclic voltammetry traces were recorded on an X-Y SEFRAM-Type TGM 164 recorder.

**X-ray crystal structure analysis**: Single crystals suitable for X-ray crystal analysis were obtained by crystallisation from a solution of **2b** in pentane at −20 °C and from a solution of **7b** at in THF at −20 °C. The unit cell constants, space-group determination and data collection were carried out on a Nonius Kappa CCD (**2b**) or an automatic CAD4 Nonius diffractometer (**7b**) with graphite-monochromatized $Mo_{K\alpha}$ radiation.[22a] The cell parameters were obtained by fitting a set of 25 high-theta reflections. After Lorentzian and polarization corrections and absorption corrections with psi scans,[22b] the structures were solved with SIR-97,[22c] which reveals non-hydrogen atoms of the structure. After anisotropic refinement, all hydrogen atoms were located in Fourier difference maps. The complete structures were refined with SHELXL97[22d] by using full-matrix least-squares techniques ($|F|$; $x, y, z, \beta_{ij}$ for C, O, P, S, Zr, and W atoms; $x, y, z$ in riding mode for the H atoms). The structures exhibit statistical disorders (80:20) between S(1)/C(10) and S(2)/C(14)S(2) for **2b** and S(2)/C(14) for **7b**. Atomic scattering factors were obtained from International Tables for X-ray Crystallography.[22e] ORTEP plots were prepared with PLATON98.[22f] All calculations were performed on a Silicon Graphics Indy computer. Crystal data and refinement parameters are given in Tables 1 and 2. Crystallographic data (excluding structure factors) for the structures reported in this paper have been deposited with the Cambridge Crystallographic Data Centre as supplementary publication no. CCDC-160751 and CCDC-160752. Copies of the data can be obtained free of charge on application to CCDC, 12 Union Road, Cambridge CB21EZ, UK (fax: (+44)1223-336-033; e-mail: deposit@ccdc.cam.ac.uk).

**1,8-Bis(2-pyridyl)octa-1,7-diyne (1a)**: Catalytic amounts of $[PdCl_2(PPh_3)_2]$ (1.19 g, 1.70 mmol) and CuI (0.32 g, 1.70 mmol) were added to a solution of 2-bromopyridine (16.2 mL, 169.9 mmol) and octa-1,7-diyne (11.2 mL, 84.9 mmol) in $Et_3N$ (170 mL) at room temperature. The heterogeneous yellow mixture was stirred for 12 h at room temperature. A precipitate formed and the mixture turned brown. All volatile materials were removed in vacuo, and the residue was extracted with $Et_2O$ (3 × 30 mL). After purification by column chromatography on silica gel (hexane/$Et_2O$ 20:80), **1a** was obtained as a bright yellow solid (yield: 20.75 g, 80 mmol, 94%). $R_f = 0.35$ (silica gel, hexane/$Et_2O$ 20:80); m.p. 60–61 °C; $^1H$ NMR (200 MHz, $CDCl_3$): $\delta = 1.74$ (m, 4H; $C{\equiv}CCH_2CH_2$), 2.42 (m, 4H; $C{\equiv}CCH_2$), 7.13 (ddd, $^3J(H,H) = 4.9$, 7.7 Hz, $^4J(H,H) = 1.0$ Hz, 2H; H5 Py), 7.32 (ddd, $^3J(H,H) = 7.7$ Hz, $^4J(H,H) = 1.0$ Hz, $^5J(H,H) = 0.9$ Hz, 2H; H3 Py), 7.55 (ddd, $^3J(H,H) = 7.7$, 7.7 Hz, $^4J(H,H) = 1.8$ Hz, 2H; H4 Py), 8.48 (ddd, $^3J(H,H) = 4.9$ Hz, $^4J(H,H) = 1.8$ Hz, $^5J(H,H) = 0.9$ Hz, 2H; H6 Py); $^{13}C\{^1H\}$ NMR (75 MHz, $CDCl_3$): $\delta = 18.9$ (s, $C{\equiv}CCH_2CH_2$), 27.5 (s, $C{\equiv}CCH_2$), 80.8 (s, $C{\equiv}CC{=}N$), 90.4 (s, $C{\equiv}C\text{-}C{=}N$), 122.4 (s, C5 Py), 126.9 (s, C3 Py), 136.1 (s, C4 Py), 143.9 (s, C2 Py), 149.8 (s, C6 Py); HR-MS (EI): $m/z$: 260.1302 $[M]^+$; calcd for $C_{18}H_{16}N_2$: 260.1313; elemental analysis (%) calcd for $C_{18}H_{16}N_2$ (260.3): C 83.05, H 6.19, N 10.76; found: C 83.10, H 6.50, N 10.48.

**2,5-Bis(2-pyridyl)zirconacyclopentadiene (2a)**: A solution of *n*-BuLi in hexane (1.6M, 1.50 mL, 2.35 mmol) was added dropwise to a solution of **1a** (0.30 g, 1.12 mmol) and $[Cp_2ZrCl_2]$ (0.33 g, 1.12 mmol) in THF (20 mL) at −78 °C. The reaction mixture was warmed to room temperature, stirred for 12 h and the solvent was removed in vacuo. The residue was washed with pentane (2 × 5 mL), and **2a** was characterized by NMR spectroscopy in solution. $^1H$ NMR (200 MHz, $CDCl_3$): $\delta = 1.55$ (m, 4H; $C{=}CCH_2CH_2$), 2.42 (m, 4H; $C{=}CCH_2$), 5.70 (s, 10H; Cp), 6.80 (ddd, $^3J(H,H) = 5.1$, 8.0 Hz, $^4J(H,H) = 1.2$ Hz, 2H; H5 Py), 6.91 (ddd, $^3J(H,H) = 8.0$ Hz, $^4J(H,H) = 1.2$ Hz, $^5J(H,H) = 1.0$ Hz, 2H; H3 Py), 7.49 (ddd, $^3J(H,H) = 8.0$, 8.0 Hz, $^4J(H,H) = 1.8$ Hz, 2H; H4 Py), 8.26 (ddd, $^3J(H,H) = 5.1$ Hz, $^4J(H,H) = 1.8$ Hz, $^5J(H,H) = 1.0$ Hz, 2H; H6 Py); $^{13}C\{^1H\}$ NMR (75 MHz, $C_6D_6$): $\delta = 24.5$ (s, $C{=}CCH_2CH_2$), 31.3 (s, $C{=}CCH_2$), 107.6 (s, Cp), 117.1 (s, C5 Py), 119.4 (s, C3 Py), 135.3 (s, C4 Py), 148.2 (s, C6 Py), 153.5 (s, $ZrC{=}C$), 169.2 (s, C2 Py), 179.8 (s, $ZrC{=}C$).

**2,5-Bis(2-thienyl)zirconacyclopentadiene (2b)**: Following the procedure described for **2a**, reaction of **1b** (0.27 g, 1.00 mmol), $[Cp_2ZrCl_2]$ (0.29 g, 1.00 mmol) and *n*-BuLi (1.6M, 0.84 mL, 2.1 mmol) afforded **2b**, which was extracted with pentane (2 × 5 mL). $^1H$ NMR (200 MHz, $C_6D_6$): $\delta = 1.55$ (m, 4H; $C{=}CCH_2CH_2$), 2.70 (m, 4H; $C{=}CCH_2$), 6.00 (s, 10H; Cp), 6.21 (dd,

$^3J$(H,H) = 3.4 Hz, $^4J$(H,H) = 1.1 Hz, 2H; H3 thienyl), 6.90 (dd, $^3J$(H,H) = 3.4 Hz, $^3J$(H,H) = 5.3 Hz, 2H; H4 thienyl), 6.96 (dd, $^3J$(H,H) = 5.3 Hz, $^4J$(H,H) = 1.1 Hz, 2H; H5 thienyl); $^{13}$C{$^1$H) NMR (75 MHz, C$_6$D$_6$): $\delta$ = 23.7 (s, C=CCH$_2$*C*H$_2$), 29.8 (s, C=C*C*H$_2$), 111.9 (s, Cp), 121.0 (s, C3 thienyl), 122.7 (s, C5 thienyl), 127.1 (s, C4 thienyl), 142.1 (s, ZrC=*C*), 149.9 (s, C2 thienyl), 177.9 (s, Zr*C*=C).

**1-Phenyl-2,5-bis(2-pyridyl)phosphole (3a)**: A solution of *n*-BuLi in hexane (1.6 M, 4.90 mL, 7.80 mmol) was added dropwise to a solution of **1a** (1.00 g, 3.73 mmol) and [Cp$_2$ZrCl$_2$] (1.10 g, 3.73 mmol) in THF (60 mL) at −78 °C. The reaction mixture was warmed to room temperature and stirred for 12 h. Freshly distilled PhPCl$_2$ (0.50 mL, 3.73 mmol) was added to this solution at −78 °C. The solution was allowed to warm to room temperature and stirred for 2 h. The solution was filtered, and the volatile materials were removed under vacuum. After purification on basic alumina (THF), **3a** was obtained as a yellow solid (yield: 1.00 g, 2.72 mmol, 73%). $R_f$ = 0.8 (alumina, THF); m.p. 192 °C; $^1$H NMR (200 MHz, C$_6$D$_6$): $\delta$ = 1.46 (m, 2H; C=CCH$_2$C*H*$_2$), 1.61 (m, 2H; C=CCH$_2$C*H*$_2$), 2.85 (m, 2H; C=CC*H*$_2$), 3.50 (m, 2H; C=CC*H*$_2$), 6.45 (ddd, $^3J$(H,H) = 4.7, 7.5 Hz, $^4J$(H,H) = 1.0 Hz, 2H; H5 Py), 6.74–6.90 (m, 3H; *m*-/*p*-H Ph), 6.97 (ddd, $^3J$(H,H) = 7.5, 7.8 Hz, $^4J$(H,H) = 1.9 Hz, 2H; H4 Py), 7.42 (dd, $^3J$(H,H) = 7.8 Hz, $^4J$(H,H) = 1.0 Hz, 2H; H3 Py), 7.69 (ddd, $^3J$(H,H) = 8.0 Hz, $^4J$(H,H) = 1.5 Hz, $^3J$(P,H) = 15.9 Hz, 2H; *o*-H Ph), 8.50 (ddd, $^3J$(H,H) = 4.7 Hz, $^4J$(H,H) = 1.9 Hz, $^5J$(H,H) = 1.0 Hz, 2H; H6 Py); $^{13}$C{$^1$H} NMR (75 MHz, CDCl$_3$): $\delta$ = 23.1 (s, C=CCH$_2$*C*H$_2$), 28.8 (s, C=C*C*H$_2$), 120.6 (s, C5 Py), 123.7 (d, $^3J$(P,C) = 9.2 Hz, C3 Py), 128.3 (d, $^3J$(P,C) = 8.1 Hz, *m*-C Ph), 128.9 (s, *p*-C Ph), 132.2 (d, $^1J$(P,C) = 12.6 Hz, ipso-C Ph), 133.8 (d, $^2J$(P,C) = 18.5 Hz, *o*-C Ph), 135.9 (d, $^4J$(P,C) = 1.2 Hz, C4 Py), 144.4 (d, $^1J$(P,C) = 4.6 Hz, P*C*=C), 148.1 (d, $^2J$(P,C) = 10.4 Hz, PC=*C*), 149.4 (s, C6 Py), 155.9 (d, $^2J$(P,C) = 19.1 Hz, C2 Py); $^{31}$P{$^1$H} NMR (81 MHz, CDCl$_3$): $\delta$ = +11.7; HR-MS (EI): *m*/*z*: 368.1451 [*M*]$^+$; calcd for C$_{24}$H$_{21}$PN$_2$: 368.1442; elemental analysis (%) calcd for C$_{24}$H$_{21}$PN$_2$ (368.42): C 78.24, H 5.75, N 7.60; found: C 78.37, H 5.88, N 7.51.

**1-Phenyl-2,5-bis(2-thienyl)phosphole (3b)**: A solution of *n*BuLi in hexane (2.5 M, 3.10 mL, 7.70 mmol) was added dropwise to a solution of [Cp$_2$ZrCl$_2$] (1.08 g, 3.70 mmol) in THF (40 mL) at −78 °C. The reaction mixture was stirred for 1 h at −78 °C, and a solution of **1b** (0.81 mL, 3.70 mmol) in THF (20 mL) was added dropwise at this temperature. The solution was warmed to room temperature and stirred for 12 h. Freshly distilled PhPBr$_2$ (0.77 mL, 3.70 mmol) was added to this solution at −78 °C. The solution was allowed to warm to room temperature and stirred for 4 h at 40 °C. The solution was filtered, and the volatile materials were removed under vacuum. Compound **3b** was isolated as an orange solid after purification on basic alumina (THF). Yield: 1.05 g, 2.77 mmol, 75%. $R_f$ = 0.7 (alumina, THF); m.p. 134 °C; $^1$H NMR (200 MHz, CD$_2$Cl$_2$): $\delta$ = 1.85 (m, 4H; C=CCH$_2$C*H*$_2$), 2.90 (m, 4H; C=CC*H*$_2$), 6.95 (ddd, $^3J$(H,H) = 5.1, 3.7 Hz, $^5J$(P,H) = 1.0 Hz, 2H; H4 thienyl), 7.08 (ddd, $^3J$(H,H) = 3.7 Hz, $^4J$(H,H) = 1.1 Hz, $^4J$(P,H) = 0.4 Hz, 2H; H3 thienyl), 7.23 (ddd, $^3J$(H,H) = 5.1 Hz, $^4J$(H,H) = 1.1 Hz, $^6J$(P,H) = 1.2 Hz, 2H; H5 thienyl), 7.25 (m, 3H; *m*-/*p*-H Ph), 7.46 (ddd, $^3J$(H,H) = 7.8, 1.6 Hz, $^3J$(P,H) = 7.8 Hz, 2H; *o*-H Ph); $^{13}$C{$^1$H} NMR (75 MHz, CDCl$_3$): $\delta$ = 23.1 (s, C=CCH$_2$*C*H$_2$), 29.3 (s, C=C*C*H$_2$), 124.8 (d, $^5J$(P,C) = 2.0 Hz, C5 thienyl), 125.6 (d, $^3J$(P,C) = 10.0 Hz, C3 thienyl) 126.8 (s, C4 thienyl), 128.7 (d, $^3J$(P,C) = 9.0 Hz, *m*-C Ph), 129.6 (s, *p*-C Ph), 133.5 (d, $^1J$(P,C) = 13.0 Hz, ipso-C Ph), 133.9 (d, $^2J$(P,C) = 19.0 Hz, *o*-C Ph), 135.7 (s, P*C*=C), 139.7 (d, $^2J$(P,C) = 22.0 Hz, C2 thienyl), 144.4 (d, $^2J$(P,C) = 9.0 Hz, PC=*C*); $^{31}$P{$^1$H} (81 MHz, CDCl$_3$): $\delta$ = +12.7; HR-MS (EI): *m*/*z*: 378.0651 [*M*]$^+$; calcd for C$_{22}$H$_{19}$PS$_2$: 378.0666; elemental analysis (%) calcd for C$_{22}$H$_{19}$PS$_2$ (378.49): C 69.82, H 5.06; found: C 69.93, H 5.31.

**1,2,5-Triphenylphosphole (3c)**: Following the procedure described for the compound **3a**, reaction of **1c** (0.30 g, 1.20 mmol), [Cp$_2$ZrCl$_2$] (0.34 g, 1.20 mmol), *n*BuLi (1.6 M, 1.50 mL, 2.40 mmol) and PhPBr$_2$ (0.30 mL, 1.44 mmol) afforded **3c** as a yellow solid after purification on basic alumina (THF). Yield: 0.24 g, 0.66 mmol, 55%. Note that with PhPCl$_2$, the yield drops to 15%. $R_f$ = 0.5 (alumina, THF); m.p. 129 °C; $^1$H NMR (200 MHz, C$_6$D$_6$): $\delta$ = 1.35 (m, 2H; C=CCH$_2$C*H*$_2$), 1.55 (m, 2H; C=CCH$_2$C*H*$_2$), 2.60 (m, 2H; C=CC*H*$_2$), 2.85 (m, 2H; C=CC*H*$_2$), 6.86 (m, 3H; *m*-/*p*-H Ph), 7.05 (m, 2H; H4 Ph), 7.22 (m, 4H; H3 Ph), 7.44 (m, 2H; *o*-H Ph), 7.59 (m, 4H; H2 Ph); $^{13}$C{$^1$H} NMR (75 MHz, CDCl$_3$): $\delta$ = 23.2 (s, C=CCH$_2$*C*H$_2$), 27.9 (s, C=C*C*H$_2$), 126.3 (s, C2 Ph), 128.4 (s, C3 Ph), 128.9 (s, *p*-C Ph), 129.3 (s, C4 Ph), 129.7 (d, $^3J$(P,C) = 8.6 Hz, *m*-C Ph), 132.7 (d, $^1J$(P,C) = 12.2 Hz, ipso-C Ph), 133.2 (d, $^2J$(P,C) = 18.0 Hz, *o*-C Ph), 137.6 (d, $^2J$(P,C) = 18.0 Hz, C1 Ph), 143.7 (d, $^1J$(P,C) = 2.4 Hz, P*C*=C), 144.2 (d, $^2J$(P,C) = 11.7 Hz, PC=*C*); $^{31}$P{$^1$H} NMR (81 MHz, CDCl$_3$): $\delta$ = +13.6; HR-MS (EI): *m*/*z*: 366.1541 [*M*]$^+$; calcd for C$_{26}$H$_{23}$PN$_2$: 366.1537; elemental analysis (%) calcd for C$_{26}$H$_{23}$PN$_2$ (366.4): C 85.22, H 6.33; found: C 85.54, H 6.01.

**1-Phenyl-2,5-bis(2-pyridyl)phosphole (3d)**: Following the procedure described for **3a**, reaction of **1d** (0.30 g, 1.21 mmol), [Cp$_2$ZrCl$_2$] (0.35 g, 1.21 mmol), *n*BuLi (1.6 M, 1.60 mL, 2.54 mmol) and PhPCl$_2$ (0.17 mL, 1.21 mmol) afforded **3d** as a yellow solid after purification on basic alumina (THF). Yield: 0.30 g, 0.85 mmol, 70%; $R_f$ = 0.7 (alumina, THF); m.p. 187 °C; $^1$H NMR (200 MHz, C$_6$D$_6$): $\delta$ = 2.05 (m, 2H; C=CCH$_2$C*H*$_2$), 2.70 (m, 2H; C=CC*H*$_2$), 3.07 (m, 2H; C=CC*H*$_2$), 6.45 (ddd, $^3J$(H,H) = 4.7, 7.4 Hz, $^4J$(H,H) = 1 Hz, 2H; H5 Py), 6.88 (t, $^3J$(H,H) = 7.3 Hz, 1H; *p*-H Ph), 6.95 (m, 4H; *m*-H Ph, H4 Py), 7.35 (ddd, $^3J$(H,H) = 8.0 Hz, $^4J$(H,H) = 1.0, $^5J$(H,H) = 0.9 Hz, 2H; H3 Py), 7.86 (ddd, $^3J$(H,H) = 8.0 Hz, $^4J$(H,H) = 1.5 Hz, $^2J$(P,H) = 15.9 Hz, 2H; *o*-H Ph), 8.47 (ddd, $^3J$(H,H) = 4.7 Hz, $^4J$(H,H) = 1.8 Hz, $^5J$(H,H) = 0.9 Hz, 2H; H6 Py); $^{13}$C{$^1$H} NMR (75 MHz, CDCl$_3$): $\delta$ = 29.2 (s, C=CCH$_2$*C*H$_2$), 30.0 (s, C=C*C*H$_2$), 120.4 (s, C5 Py), 121.7 (d, $^3J$(P,C) = 7.8 Hz, C3 Py), 128.2 (s, *p*-C Ph), 128.4 (d, $^3J$(P,C) = 8.1 Hz, *m*-C Ph), 134.2 (d, $^2J$(P,C) = 18.8 Hz, *o*-C Ph), 139.0 (s, C4 Py), 139.6 (s, P*C*=C), 149.6 (s, C6 Py), 156.7 (d, $^2J$(P,C) = 19.6 Hz, C2 Py), 158.3 (d, $^2J$(P,C) = 10.2 Hz, PC=*C*), ipso-C of Ph was not observed; $^{31}$P{$^1$H} NMR (81 MHz, CDCl$_3$): $\delta$ = +36.0; HR-MS (EI): *m*/*z*: 354.1275 [*M*]$^+$; calcd for C$_{23}$H$_{19}$PN$_2$: 354.1286; elemental analysis (%) calcd for C$_{23}$H$_{19}$PN$_2$ (354.39): C 77.95, H 5.40, N 7.90; found: C 78.10, H 5.28, N 7.78.

**1-Isopropyl-2,5-bis(2-pyridyl)phosphole (3e)**: Following the procedure described for **3a**, reaction of **1a** (0.26 g, 1.00 mmol), [Cp$_2$ZrCl$_2$] (0.29 g, 1.00 mmol), *n*-BuLi (2.5 M, 0.85 mL, 2.10 mmol) and *i*PrPCl$_2$ (0.15 mL, 1.20 mmol) afforded **3e** as a yellow solid (yield: 0.20 g, 0.60 mmol, 60%). M.p. 52 °C; $^1$H NMR (200 MHz, CDCl$_3$): $\delta$ = 0.75 (dd, $^3J$(H,H) = 7.1 Hz, $^3J$(P,H) = 13.1 Hz, 6H; CHC*H*$_3$), 1.70 (m, 4H; C=CCH$_2$C*H*$_2$), 2.15 (sept d, $^3J$(H,H) = 7.1 Hz, $^2J$(P,H) = 3.4 Hz, 1H; C*H*CH$_3$), 2.60 (m, 2H; C=CC*H*$_2$), 3.57 (m, 2H; C=CC*H*$_2$), 7.03 (ddd, $^3J$(H,H) = 4.9, 7.8 Hz, $^4J$(H,H) = 1.3 Hz, 2H; H5 Py), 7.46 (d, $^3J$(H,H) = 7.8 Hz, 2H; H3 Py), 7.61 (ddd, $^3J$(H,H) = 7.8, 7.8 Hz, $^4J$(H,H) = 1.8 Hz, 2H; H4 Py), 8.60 (ddd, $^3J$(H,H) = 4.9 Hz, $^4J$(H,H) = 1.8 Hz, $^5J$(H,H) = 0.9 Hz, 2H; H6 Py); $^{13}$C{$^1$H} NMR (75 MHz, CDCl$_3$): $\delta$ = 19.7 (d, $^2J$(P,C) = 6.3 Hz, CH*C*H$_3$), 23.2 (s, C=CCH$_2$*C*H$_2$), 26.9 (d, $^1J$(P,C) = 15.6 Hz, *C*HCH$_3$), 28.2 (s, C=C*C*H$_2$), 120.4 (s, C5 Py), 123.8 (d, $^3J$(P,C) = 7.8 Hz, C3 Py), 135.9 (d, $^4J$(P,C) = 1.6 Hz, C4 Py), 143.2 (s, P*C*=C), 147.3 (d, $^2J$(P,C) = 8.6 Hz, PC=*C*), 149.5 (d, $^4J$(P,C) = 1.6 Hz, C6 Py), 157.0 (d, $^2J$(P,C) = 18.8 Hz, C2 Py); $^{31}$P{$^1$H} NMR (81 MHz, CDCl$_3$): $\delta$ = +30.5; HR-MS (EI): *m*/*z*: 334.1607 [*M*]$^+$; calcd for C$_{21}$H$_{23}$PN$_2$: 334.1599; elemental analysis (%) calcd for C$_{21}$H$_{23}$PN$_2$ (334.40): C 75.43, H 6.93, N 8.35; found: C 75.62, H 7.08, N 8.23.

**1-Diisopropylamino-2,5-bis(2-pyridyl)phosphole (3f)**: A solution of *n*BuLi in hexane (2.5 M, 1.30 mL, 3.15 mmol) was added dropwise to a solution of **1a** (0.39 g, 1.50 mmol) and [Cp$_2$ZrCl$_2$] (0.44 g, 1.50 mmol) in THF (20 mL) at −78 °C. The reaction mixture was warmed to room temperature and stirred for 12 h. Freshly distilled PCl$_3$ (0.16 mL, 1.80 mmol) was added to this solution at −78 °C. The solution was allowed to warm to room temperature and stirred for 1 h, then freshly distilled *i*Pr$_2$NH (0.25 mL, 1.80 mmol) was added dropwise at −20 °C. The solution was allowed to warm to room temperature and stirred for 4 h. All volatile materials were removed in vacuo, and the residue was extracted with pentane (3 × 10 mL). The product was obtained as a yellow solid (yield: 0.32 g, 0.94 mmol, 45%). M.p. 182 °C (decomp); $^1$H NMR (200 MHz, C$_6$D$_6$): $\delta$ = 0.55 (d, $^3J$(H,H) = 6.0 Hz, 6H; CHC*H*$_3$), 1.25 (m, 8H; C=CCH$_2$C*H*$_2$, CHC*H*$_3$), 1.55 (m, 2H; C=CCH$_2$C*H*$_2$), 2.55 (m, 2H; C=CC*H*$_2$), 2.93 (m, 2H; C=CC*H*$_2$), 3.50 (m, 2H; NC*H*CH$_3$), 6.64 (ddd, $^3J$(H,H) = 4.7, 7.5 Hz, $^4J$(H,H) = 1.0 Hz, 2H; H5 Py), 7.22 (dd, $^3J$(H,H) = 7.5, 7.9 Hz, $^4J$(H,H) = 2.0 Hz, 2H; H4 Py), 7.52 (dd, $^3J$(H,H) = 7.9 Hz, $^4J$(H,H) = 1 Hz, 2H; H3 Py), 8.50 (ddd, $^3J$(H,H) = 4.7 Hz, $^4J$(H,H) = 2.0 Hz, $^5J$(H,H) = 0.9 Hz, 2H; H6 Py); $^{13}$C{$^1$H} NMR (75 MHz, CDCl$_3$): $\delta$ = 22.8 (d, $^3J$(P,C) = 9.5 Hz, CH*C*H$_3$), 23.2 (s, C=CCH$_2$*C*H$_2$), 26.3 (d, $^3J$(P,C) = 9.5 Hz, CH*C*H$_3$), 27.8 (s, C=C*C*H$_2$), 47.9 (d, $^2J$(P,C) = 14.9 Hz, N*C*H), 119.9 (s, C5 Py), 124.2 (d, $^3J$(P,C) = 9.3 Hz, C3 Py), 134.8 (s, C4 Py), 144.2 (d, $^3J$(P,C) = 12.6 Hz, PC=*C*), 144.4 (s, P*C*=C), 149.5 (d, $^3J$(P,C) = 1.6 Hz, C6 Py), 157.2 (d, $^2J$(P,C) = 20.0 Hz, C2 Py); $^{31}$P{$^1$H} NMR (81 MHz, CDCl$_3$): $\delta$ = +45.3.

**1-Phenyl-2,5-bis(2-thienyl)oxophosphole (4b)**: A solution of bis(trimethylsilyl) peroxide (2.3 mL, 0.53 mmol) in CH$_2$Cl$_2$ (10 mL) was added at room temperature to a solution of phosphole **3b** (0.20 g, 0.53 mmol) in CH$_2$Cl$_2$ (10 mL). The solution was stirred for 12 h. The volatile substances were removed under vacuum, and the residue was washed with pentane (3 ×

10 mL). Compound **4b** was obtained as an orange solid (yield: 0.20 g, 0.50 mmol, 95%). M.p. 227 °C; $^1$H NMR (200 MHz, CDCl$_3$): $\delta = 1.85$ (m, 4H; C=CCH$_2$C$H_2$), 2.85 (m, 4H; C=CC$H_2$), 6.96 (dd, $^3J$(H,H) = 3.8, 5.1 Hz, 2H; H4 thienyl), 7.29 (ddd, $^3J$(H,H) = 5.1 Hz, $^4J$(H,H) = 1.6, $^5J$(P,H) = 0.8 Hz, 2H; H5 thienyl), 7.38 (m, 5H; *m*-/*p*-H Ph, H3 thienyl) 7.78 (ddd, $^3J$(H,H) = 7.3 Hz, $^4J$(H,H) = 1.5 Hz, $^3J$(P,H) = 12.3 Hz, 2H; *o*-H Ph); $^{13}$C{$^1$H) NMR (75 MHz, CDCl$_3$): $\delta = 22.4$ (s, C=CCH$_2$$C$H$_2$), 28.6 (d, $^3J$(P,C) = 14.8 Hz, C=C$C$H$_2$), 125.0 (d, $^1J$(P,C) = 98.6 Hz, P$C$=C), 126.7 (s, C5 thienyl), 127.4 (s, C4 thienyl), 127.8 (d, $^3J$(P,C) = 4.7 Hz, C3 thienyl), 128.9 (d, $^3J$(P,C) = 12.4 Hz, *m*-C Ph), 130.1 (d, $^1J$(P,C) = 94.7 Hz, ipso-C Ph), 130.6 (d, $^2J$(P,C) = 10.1 Hz, ipso-C Ph), 132.1 (d, $^4J$(P,C) = 2.3 Hz, *p*-C Ph), 135.5 (d, $^2J$(P,C) = 16.0 Hz, C2 thienyl), 145.1 (d, $^2J$(P,C) = 24.2 Hz, PC=$C$); $^{31}$P{$^1$H) NMR (81 MHz, CDCl$_3$): $\delta = +42.3$; HR-MS (EI): *m*/*z*: 394.0615 $[M]^+$; calcd for $C_{22}H_{19}S_2PO$: 394.0605; elemental analysis (%) calcd for $C_{22}H_{19}S_2PO$ (394.48): C 66.98, H 4.85; found: C 66.83, H 4.78.

**1-Phenyl-2,5-bis(2-pyridyl)thiooxophosphole (5a)**: Elemental sulfur (35 mg, 1.10 mmol) was added to a solution of phosphole **3a** (0.40 g, 1.10 mmol) in THF (15 mL) at room temperature. The reaction mixture was stirred for 36 h, filtered, and the solvent was removed in vacuo. After purification on silica gel, **5a** was obtained as a yellow solid (yield: 0.40 g, 1.0 mmol, 92%). $R_f = 0.15$ (silica gel, diethyl ether/hexane 80:20); m.p. 114 °C; $^1$H NMR (200 MHz, C$_6$D$_6$): $\delta = 1.81$ (m, 4H; C=CCH$_2$C$H_2$), 3.17 (m, 2H; C=CC$H_2$), 3.65 (m, 2H; C=CC$H_2$), 7.08 (ddd, $^3J$(H,H) = 4.8, 7.6 Hz, $^4J$(H,H) = 1.0 Hz, 2H; H5 Py), 7.35–7.45 (m, 3H; *m*-/*p*-H Ph), 7.55 (ddd, $^3J$(H,H) = 7.6, 7.6 Hz, $^4J$(H,H) = 1.9 Hz, 2H; H4 Py), 7.68 (dd, $^3J$(H,H) = 7.6 Hz, $^4J$(H,H) = 1.0 Hz, 2H; H3 Py), 7.88 (ddd, $^3J$(H,H) = 8.0 Hz, $^4J$(H,H) = 1.4 Hz, $^5J$(P,H) = 14.0 Hz, 2H; *o*-H Ph), 8.54 (ddd, $^3J$(H,H) = 4.8 Hz, $^4J$(H,H) = 1.9 Hz, $^5J$(H,H) = 0.9 Hz, 2H; H6 Py); $^{13}$C{$^1$H} NMR (75 MHz, CDCl$_3$): $\delta = 22.5$ (s, C=CCH$_2$$C$H$_2$), 29.4 (d, $^3J$(P,C) = 12.6 Hz, C=C$C$H$_2$), 122.1 (s, C5 Py), 124.4 (d, $^3J$(P,C) = 2.9 Hz, C3 Py), 128.6 (d, $^1J$(P,C) = 75.5 Hz, ipso-C Ph), 128.8 (d, $J$(P,C) = 12.6 Hz, *o*-C or *m*-C Ph), 130.8 (d, $J$(P,C) = 11.7 Hz, *o*-C or *m*-C Ph), 131.7 (d, $^4J$(P,C) = 3.0 Hz, *p*-C Ph), 132.9 (d, $^1J$(P,C) = 83.0 Hz, P$C$=C), 135.9 (s, C4 Py), 149.4 (d, $^4J$(P,C) = 1.1 Hz, C6 Py), 152.1 (d, $^2J$(P,C) = 17.3 Hz, PC=$C$), 153.0 (d, $^2J$(P,C) = 20.4 Hz, C2 Py); $^{31}$P{$^1$H} NMR (81 MHz, CDCl$_3$): $\delta = +53.1$; HR-MS (EI): *m*/*z*: 400.1186 $[M]^+$; calcd for $C_{24}H_{21}PN_2S$: 400.1163; elemental analysis (%) calcd for $C_{24}H_{21}PN_2S$ (400.48): C 71.98, H 5.29, N 6.99; found: C 72.12, H 5.40, N 7.02.

**1-Phenyl-2,5-bis(2-thienyl)thiooxophosphole (5b)**: Elemental sulfur (17 mg, 0.53 mmol) was added to a solution of phosphole **3b** (0.20 g, 0.53 mmol) in THF (15 mL) at room temperature. The reaction mixture was stirred for 36 h, filtered, and the solvent was removed in vacuo. After purification on silica gel, **5b** was obtained as a yellow solid (yield: 0.40 g, 0.97 mmol, 93%). $R_f = 0.7$ (silica gel, diethyl ether/hexane 80:20); m.p. 114 °C, $^1$H NMR (200 MHz, CD$_2$Cl$_2$): $\delta = 1.80$ (m, 4H; C=CCH$_2$C$H_2$), 2.85 (m, 2H; C=CC$H_2$), 3.65 (m, 2H; C=CC$H_2$), 6.98 (dd, $^3J$(H,H) = 5.1, 3.7 Hz, 2H; H4 thienyl), 7.34 (dd, $^3J$(H,H) = 5.1 Hz, $^4J$(H,H) = 1.1 Hz, 2H; H5 thienyl), 7.37 (ddd, $^3J$(H,H) = 3.7 Hz, $^4J$(H,H) = 1.1 Hz, $^4J$(P,H) = 1.0 Hz, 2H; H3 thienyl), 7.45 (m, 3H; *m*-/*p*-H Ph), 7.90 (ddd, $^3J$(H,H) = 8.0 Hz, $^4J$(H,H) = 1.4 Hz, $^3J$(P,H) = 9.0 Hz, 2H; *o*-H Ph); $^{13}$C{$^1$H) NMR (75 MHz, CDCl$_3$): $\delta = 22.5$ (s, C=CCH$_2$$C$H$_2$), 29.2 (d, $^3J$(P,C) = 13.3 Hz, C=C$C$H$_2$), 126.8 (s, C5 thienyl), 127.4 (s, C4 thienyl), 127.8 (d, $^3J$(P,C) = 5.5 Hz, C3 thienyl), 128.5 (d, $^1J$(P,C) = 83.7 Hz, P$C$=C), 128.9 (d, $^1J$(P,C) = 73.9 Hz, ipso-C Ph), 129.0 (d, $^3J$(P,C) = 12.5 Hz, *m*-C Ph), 130.7 (d, $^2J$(P,C) = 11.7 Hz, *o*-C Ph), 132.1 (d, $^4J$(P,C) = 3.0 Hz, *p*-C Ph), 134.7 (d, $^2J$(P,C) = 17.5 Hz, C2 thienyl), 146.1 (d, $^2J$(P,C) = 20.9 Hz, PC=$C$); $^{31}$P{$^1$H) NMR (81 MHz, CDCl$_3$): $\delta = +52.6$; HR-MS (EI): *m*/*z*: 410.0403 $[M]^+$; calcd for $C_{22}H_{19}PS_3$: 410.0387; elemental analysis (%) calcd for $C_{22}H_{19}PS_3$ (410.55): C 64.36, H 4.36; found: C 64.12, H 4.22.

**1-Phenyl-2,5-bis(2-thienyl)selenoxophosphole (6b)**: A solution of phosphole **3b** (0.10 g, 0.26 mmol) and elemental selenium (0.02 g, 0.26 mmol) in THF (10 mL) was stirred for 24 h at room temperature. The solvent was removed under vacuum, and the residue was washed with pentane (3 × 10 mL). Compound **6b** was obtained as an orange solid (yield: 0.11 g, 0.24 mmol, 91%). $^1$H NMR (200 MHz, CD$_2$Cl$_2$): $\delta = 1.80$ (m, 4H; C=CCH$_2$C$H_2$), 2.90 (m, 4H; C=CC$H_2$), 6.90 (ddd, $^3J$(H,H) = 3.7, 5.1 Hz, $^5J$(P,H) = 0.5 Hz, 2H; H4 thienyl), 7.32 (ddd, $^3J$(H,H) = 5.1 Hz, $^4J$(H,H) = 1.0 Hz, $^5J$(P,H) = 1.0 Hz, 2H; H5 thienyl), 7.35 (dd, $^3J$(H,H) = 3.7 Hz, $^4J$(H,H) = 1.0 Hz, 2H; H3 thienyl), 7.42 (m, 3H; *m*-/*p*-H Ph), 7.90 (ddd, $^3J$(H,H) = 8.1 Hz, $^4J$(H,H) = 1.5 Hz, $^3J$(P,H) = 14.2 Hz, 2H; *o*-H Ph); $^{13}$C{$^1$H) NMR (75 MHz, CDCl$_3$): $\delta = 22.4$ (s, C=CCH$_2$$C$H$_2$), 29.4 (d, $^3J$(P,C) = 12.5 Hz, C=C$C$H$_2$), 125.8 (d, $^1J$(P,C) = 74.3 Hz, P$C$=C), 126.9 (s, C5 thienyl), 127.0 (d, $^4J$(P,C) = 9.4 Hz, C4 thienyl), 127.8 (d, $^3J$(P,C) = 5.5 Hz, C3 thienyl), 128.9 (d, $^3J$(P,C) = 12.5 Hz, *m*-C Ph), 131.2 (d, $^2J$(P,C) = 11.7 Hz, *o*-C Ph), 132.2 (d, $^4J$(P,C) = 3.1 Hz, *p*-C Ph), 134.8 (d, $^2J$(P,C) = 17.2 Hz, C2 thienyl), 145.6 (d, $^2J$(P,C) = 20.8 Hz, PC=$C$), ipso-C was not observed; $^{31}$P{$^1$H) NMR (81 MHz, CDCl$_3$): $\delta = +41.5$ ($^1J$(P,Se) = 372.2 Hz); HR-MS (EI): *m*/*z*: 457.9878 $[M]^+$; calcd for $C_{22}H_{19}S_2PSe$: 457.9928; elemental analysis (%) calcd for $C_{22}H_{19}S_2PSe$ (457.45): C 57.76, H 4.19; found: C 57.44, H 4.22.

**1-Phenyl-2,5-bis(2-pyridyl)phosphole W(CO)$_5$ complex (7a)**: A solution of [W(CO)$_5$(thf)] (0.19 mg, 0.54 mmol) in THF (15 mL) was added dropwise to a solution of phosphole **3a** (0.20 g, 0.54 mmol) in THF (10 mL) at room temperature. The solution was stirred for 3 h, then the solvent was removed in vacuo, and **7a** was crystallized from THF at −35 °C as yellow crystals (yield: 0.35 g, 1.37 mmol, 95%). M.p. 204 °C (decomp); $^1$H NMR (200 MHz, C$_6$D$_6$): $\delta = 1.40$ (m, 4H; C=CCH$_2$C$H_2$), 2.90 (m, 2H; C=CC$H_2$), 3.15 (m, 2H; C=CC$H_2$), 6.45 (ddd, $^3J$(H,H) = 4.7, 7.3 Hz, $^4J$(H,H) = 1.0 Hz, 2H; H5 Py), 7.20–7.31 (m, 5H; *m*-/*p*-H Ph, H3 Py), 7.89 (ddd, $^3J$(H,H) = 7.8, 7.3 Hz, $^4J$(H,H) = 1.8 Hz, 2H; H4 Py), 7.88 (m, 2H; *o*-H Ph), 8.43 (ddd, $^3J$(H,H) = 4.7 Hz, $^4J$(H,H) = 1.8 Hz, $^5J$(H,H) = 1.0 Hz, 2H; H6 Py); $^{13}$C{$^1$H} NMR (75 MHz, CDCl$_3$): $\delta = 22.8$ (s, C=CCH$_2$$C$H$_2$), 29.6 (d, $^3J$(P,C) = 7.1 Hz, C=C$C$H$_2$), 121.6 (s, C5 Py), 123.4 (d, $^3J$(P,C) = 4.9 Hz, C3 Py), 128.5 (d, $J$(P,C) = 10.7 Hz, *o*-C or *m*-C Ph), 132.4 (d, $J$(P,C) = 12.8 Hz, *o*-C or *m*-C Ph), 130.1 (d, $^4J$(P,C) = 2.3 Hz, *p*-C Ph), 131.2 (d, $^1J$(P,C) = 41.2 Hz, ipso-C Ph), 144.0 (d, $^1J$(P,C) = 45.0 Hz, P$C$=C), 135.9 (s, C4 Py), 149.0 (s, C6 Py), 148.3 (d, $^2J$(P,C) = 11.2 Hz, P-C=$C$), 153.0 (d, $^2J$(P,C) = 13.6 Hz, C2 Py), 197.3 (d, $^1J$(P,C) = 6.9 Hz, $^1J$(W,C) = 126.7 Hz, CO$_{eq}$), 199.7 (d, $J$(P,C) = 21.6 Hz, CO$_{ax}$); $^{31}$P{$^1$H} NMR (81 MHz, CDCl$_3$): $\delta = +30.2$ ($^1J$(P,W) = 231.8 Hz); HR-MS (FAB, *m*NBA): *m*/*z*: 693.0786 $[M+H]^+$; calcd for $C_{29}H_{22}PN_2O_5W$: 693.0776; elemental analysis (%) calcd for $C_{29}H_{21}PN_2O_5W$ (692.32): C 50.31, H 3.06, N 4.05; found: C 50.22, H 3.00, N 4.08.

**1-Phenyl-2,5-bis(2-thienyl)phosphole W(CO)$_5$ complex (7b)**: A solution of [W(CO)$_5$(thf)] (0.20 mg, 0.54 mmol) in THF (10 mL) was added dropwise to a solution of phosphole **3b** (0.20 g, 0.54 mmol) in THF (15 mL) at room temperature. The solution was stirred for 15 h. The solvent was removed in vacuo, and **7b** was crystallized from THF at −20 °C as yellow crystals (yield: 0.33 g, 0.48 mmol, 96%). M.p. 204 °C (decomp); $^1$H NMR (200 MHz, C$_6$D$_6$): $\delta = 1.35$ (m, 4H; C=CCH$_2$C$H_2$), 2.67 (m, 4H; C=CC$H_2$), 6.62 (ddd, $^3J$(H,H) = 3.7, 5.1 Hz, $^5J$(P,H) = 0.5 Hz, 2H; H4 thienyl), 6.82 (ddd, $^3J$(H,H) = 5.1 Hz, $^4J$(H,H) = 1.0 Hz, $^4J$(P,H) = 0.9 Hz, 2H; H5 thienyl), 6.92 (ddd, $^3J$(H,H) = 3.7 Hz, $^4J$(H,H) = 1.0 Hz, $^4J$(P,H) = 0.9 Hz, 2H; H3 thienyl), 7.02 (m, 3H; *m*-/*p*-H Ph), 7.78 (ddd, $^3J$(H,H) = 8.1 Hz, $^4J$(H,H) = 1.5 Hz, $^3J$(P,H) = 11.7 Hz, 2H; *o*-H Ph); $^{13}$C{$^1$H} NMR (75 MHz, CDCl$_3$): $\delta = 22.8$ (s, C=CCH$_2$$C$H$_2$), 28.7 (d, $^3J$(P,C) = 7.6 Hz, C=C$C$H$_2$), 126.4 (s, C5 thienyl), 127.0 (s, C4 thienyl), 127.5 (d, $^3J$(P,C) = 5.5 Hz, C3 thienyl), 128.0 (d, $^1J$(P,C) = 79.0 Hz, ipso-C Ph), 129.4 (d, $^3J$(P,C) = 10.9 Hz, *m*-C Ph), 131.6 (d, $^4J$(P,C) = 2.3 Hz, *p*-C Ph), 133.4 (d, $^2J$(P,C) = 13.3 Hz, *o*-C Ph), 136.2 (d, $^2J$(P,C) = 18.0 Hz, C2 thienyl), 136.8 (d, $^1J$(P,C) = 43.5 Hz, P$C$=C), 144.2 (d, $^2J$(P,C) = 13.3 Hz, PC=$C$), 196.2 (d, $^2J$(P,C) = 6.3, $^1J$(W,C) = 127.8 Hz, CO$_{eq}$), 198.2 (d, $^2J$(P,C) = 21.4 Hz, CO$_{ax}$); $^{31}$P{$^1$H} NMR (81 MHz, CDCl$_3$): $\delta = +33.4$ ($^1J$(P,W) = 226.2 Hz); HR-MS (EI): *m*/*z*: 701.9943 $[M]^+$; calcd for $C_{27}H_{19}PS_2O_5W$: 701.9921; elemental analysis (%) calcd for $C_{27}H_{19}PS_2O_5W$ (702.39): C 46.17, H 2.73; found: C 46.36, H 2.71.

**1-Methyl-1-phenyl-2,5-bis(2-pyridyl)phospholium salt (8a)**: Methyl trifluoromethanesulfonate (0.075 g, 0.45 mmol, 0.8 equiv) was added to a solution of phosphole **3a** (0.21 g, 0.57 mmol) in dichloromethane (10 mL) at room temperature. This solution was stirred for 6 h at room temperature. The volatile materials were removed under vacuum. The residue was washed with toluene (3 × 5 mL), and **8a** was obtained as a yellow solid (yield: 0.31 g, 0.57 mmol, 75%). $^1$H NMR (200 MHz, CDCl$_3$): $\delta = 1.90$ (m, 4H; C=CCH$_2$C$H_2$), 2.80 (d, $^2J$(P,H) = 15.2 Hz, 3H; C$H_3$), 3.10 (m, 4H; C=CC$H_2$), 7.15 (m, 2H; H5 Py), 7.43 (m, 3H; *m*-/*p*-H Ph), 7.73 (m, 6H; *o*-H Ph, H3 and H5 Py), 8.40 (ddd, $^3J$(H,H) = 4.7 Hz, $^4J$(H,H) = 1.7 Hz, $^5J$(H,H) = 1.1 Hz, 2H; H6 Py); $^{13}$C (75 MHz, CDCl$_3$): $\delta = 9.54$ (d, $^1J$(P,C) = 57.1 Hz, $C$H$_3$), 21.4 (s, C=CCH$_2$$C$H$_2$), 30.3 (d, $^3J$(P,C) = 13.8 Hz, C=C$C$H$_2$), 119.8 (d, $^1J$(P,C) = 91.4 Hz, ipso-C Ph), 123.6 (s, C5 Py), 123.8 (d, $^3J$(P,C) = 8.3 Hz, C3 Py), 128.6 (d, $^1J$(P,C) = 87.0 Hz, P$C$=C), 129.7 (d, $^3J$(P,C) = 13.9 Hz, *m*-C Ph), 131.4 (d, $^2J$(P,C) = 11.1 Hz, *o*-C Ph), 133.7 (d, $^4J$(P,C) = 3.3 Hz, *p*-C Ph), 137.7 (d, $^4J$(P,C) = 1.3 Hz, C4 Py), 149.3 (s, C6

Py), 149.9 (d, $^{2}J$(P,C) = 8.6 Hz, C2 Py), 157.4 (d, $^{2}J$(P,C) = 20.4 Hz, $\mathrm{PC{=}}\mathit{C}$); $^{31}$P (121.496 MHz, $\mathrm{CDCl_3}$): $\delta = +41.4$. HR-MS (FAB, *m*NBA): *m*/*z*: 383.1677 $[M - \mathrm{OTf}]^+$; calcd for $\mathrm{C_{25}H_{24}PN_2}$: 383.1677.

**1-Methyl-1-phenyl-2,5-bis(2-thienyl)phospholium trifluoromethanesulfonate (8b)**: Methyl trifluoromethanesulfonate (0.10 g, 0.6 mmol) was added at room temperatute to a solution of phosphole **3b** (0.23 g, 0.6 mmol) in dichloromethane (10 mL). The solution was stirred for 1 h at room temperature. The volatile materials were removed under vacuum, and the residue was washed with diethyl ether (3 × 10 mL). Compound **8b** was obtained as a red solid (yield: 0.23 g, 0.42 mmol, 95 %). M.p. 143 °C; $^{1}$H NMR (200 MHz, $\mathrm{CDCl_3}$): $\delta = 1.90$ (m, 4H; $\mathrm{C{=}CCH_2}\mathit{CH_2}$), 2.60 (d, $^{2}J$(P,H) = 13.8 Hz, 3H; $\mathit{CH_3}$), 3.00 (m, 4H; $\mathrm{C{=}C}\mathit{CH_2}$), 6.99 (m, 4H; H4, H3 thienyl), 7.41 (ddd, $^{3}J$(H,H) = 5.0 Hz, $^{4}J$(H,H) = 1.5 Hz, $^{5}J$(P,H) = 1.2 Hz, 2H; H5 thienyl), 7.66 (m, 3H; *m*-/*p*-H Ph), 7.93 (ddd, $^{3}J$(H,H) = 6.2 Hz, $^{4}J$(H,H) = 1.5 Hz, $^{3}J$(P,H) = 14.4 Hz, 2H; *o*-H Ph); $^{13}$C{$^{1}$H) NMR (75 MHz, $\mathrm{CDCl_3}$): $\delta = 5.50$ (d, $^{1}J$(P,C) = 50.1 Hz, $\mathrm{CH_3}$), 21.6 (s, $\mathrm{C{=}CCH_2}\mathit{C}\mathrm{H_2}$), 29.9 (d, $^{3}J$(P,C) = 13.4 Hz, $\mathrm{C{=}}\mathit{C}\mathrm{H_2}$), 115.6 (d, $^{1}J$(P,C) = 79.9 Hz, ipso-C Ph), 118.4 (d, $^{1}J$(P,C) = 85.3 Hz, $\mathrm{P}\mathit{C}\mathrm{{=}C}$), 128.6 (s, C5 thienyl), 128.7 (d, $^{3}J$(P,C) = 6.1 Hz, C3 thienyl), 129.4 (s, C4 thienyl), 131.2 (d, $^{3}J$(P,C) = 12.2 Hz, *m*-C Ph), 131.8 (d, $^{2}J$(P,C) = 15.9 Hz, C2 thienyl), 132.4 (d, $^{2}J$(P,C) = 12.2 Hz, *o*-C Ph), 135.9 (d, $^{4}J$(P,C) = 3.6 Hz, *p*-C Ph), 154.1 (d, $^{2}J$(P,C) = 20.8 Hz, $\mathrm{PC{=}}\mathit{C}$); $^{31}$P{$^{1}$H) NMR (81 MHz, $\mathrm{CDCl_3}$): $\delta = +34.8$; HR-MS (FAB, *m*NBA): *m*/*z*: 393.0901 $[M - \mathrm{OTf}]^+$; calcd for $\mathrm{C_{23}H_{22}S_2P}$ 393.0901; elemental analysis (%) calcd for $\mathrm{C_{24}H_{22}S_3PF_30_3}$ (542.59): C 53.13, H 4.09; found: C 53.24, H 4.00.

**1-(2-Thienyl)octa-1,7-diyne (9)**: Catalytic amounts of $[\mathrm{Pd(PPh_3)_2Cl_2}]$ (130 mg, 0.18 mmol) and CuI (36 mg, 0.18 mmol) were added to a solution of 2-iodothiophene (1.03 mL, 9.4 mmol) and octa-1,7-diyne (1.25 mL, 1.0 g, 9.4 mmol) in triethylamine (35 mL) at room temperature. The heterogeneous yellow mixture was stirred for 7 h at room temperature. The reaction mixture turned brown and a large amount of precipitate formed during the course of the reaction. All volatile materials were removed in vacuo, and the residue was extracted with $\mathrm{Et_2O}$ (3 × 30 mL). Then the solvent was removed, and the crude oil was purified by column chromatography (silica gel, heptane). Compound **9** was obtained as a translucent oil (yield: 0.6 g, 3.19 mmol, 34 %). $^{1}$H NMR (200 MHz, $\mathrm{CDCl_3}$): $\delta = 1.68$ (m, 4H; $\mathrm{C{\equiv}CCH_2}\mathit{CH_2}$), 1.98 (t, $^{3}J$(H,H) = 2.6 Hz, 1H; $\mathrm{C{\equiv}C}\mathit{H}$), 2.22 (m, 2H; $\mathrm{C{\equiv}C}\mathit{CH_2}$), 2.44 (m, 2H; $\mathrm{C{\equiv}C}\mathit{CH_2}$), 6.92 (dd, $^{3}J$(H,H) = 5.12 Hz, $^{3}J$(H,H) = 3.7 Hz, 1H; H4 thienyl), 7.14 (dd, $^{3}J$(H,H) = 3.7 Hz, $^{4}J$(H,H) = 1.1 Hz, 1H; H3 thienyl), 7.16 (dd, $^{3}J$(H,H) = 5.1 Hz, $^{4}J$(H,H) = 1.1 Hz, 1H; H5 thienyl); $^{13}$C{$^{1}$H} NMR (75 MHz, $\mathrm{CDCl_3}$): $\delta = 18.1$ (s, $\mathrm{C{\equiv}CCH_2}\mathit{C}\mathrm{H_2}$), 19.3 (s, $\mathrm{C{\equiv}CCH_2}\mathit{C}\mathrm{H_2}$), 27.6 (s, $\mathrm{C{\equiv}}\mathit{C}\mathrm{CH_2}$), 27.7 (s, $\mathrm{C{\equiv}C}\mathit{C}\mathrm{H_2}$), 68.9 (s, $\mathrm{C{\equiv}}\mathit{C}\mathrm{H}$), 74.3 (s, $\mathrm{C{\equiv}}\mathit{C}\mathrm{CS}$), 84.1 (s, $\mathit{C}\mathrm{{\equiv}C\text{-}H}$), 93.9 (s, $\mathit{C}\mathrm{{\equiv}CCS}$), 124.2 (s, C2 thienyl), 126.1 (s, C4 thienyl), 126.9 (s, C5 thienyl), 131.1 (s, C3 thienyl); FT-IR ($\mathrm{CH_2Cl_2}$): $\tilde{\nu} = 3304\ \mathrm{cm^{-1}}$ (s; $\mathrm{C{\equiv}CH}$); HR-MS (EI): *m*/*z*: 188.0690 $[M]^+$; calcd for $\mathrm{C_{12}H_{12}S}$: 188.0660; elemental analysis (%) calcd for $\mathrm{C_{12}H_{12}S}$ (188.29): C 76.55, H 6.42; found: C 76.78, H 6.15.

**5,5′-Bis[8-(2-thienyl)octa-1,7-diyne]-2,2′-dithienyl (10)**: Catalytic amounts of $[\mathrm{Pd(PPh_3)_2Cl_2}]$ (0.019 g, 0.027 mmol) and CuI (0.013 g, 0.067 mmol) were added to a solution of 5,5′-dibromo-2,2′-dithienyl (0.22 g, 0.68 mmol) and 1-(2-thienyl)octa-1,7-diyne (0.26 g, 1.36 mmol) in $\mathrm{Et_3N}$ (15 mL) and toluene (6 mL) at room temperature. The heterogeneous yellow mixture was stirred for 2 d at room temperature. A precipitate formed and the mixture turned black. All volatile materials were removed in vacuo, and the residue was extracted with $\mathrm{Et_2O}$ (3 × 30 mL). After purification by column chromatography on silica gel (heptane/$\mathrm{Et_2O}$ 99.9:0.1), **10** was obtained as a yellowish solid (yield: 0.34 g, 0.62 mmol, 92 %). $^{1}$H NMR (200 MHz, $\mathrm{CDCl_3}$): $\delta = 1.70$ (m, 8H; $\mathrm{C{\equiv}CCH_2}\mathit{CH_2}$), 2.50 (m, 8H; $\mathrm{C{\equiv}C\text{-}}\mathit{CH_2}$), 6.91 (dd, $^{3}J$(H,H) = 5.1 Hz, $^{3}J$(H,H) = 3.7 Hz, 2H; H4 thienyl), 6.98 (AB system, $J$(H,H) = 3.8 Hz, $\nu_0\delta = 7.4$ Hz, 4H; H3′ and H4′ thienyl), 7.09 (dd, $^{3}J$(H,H) = 3.7 Hz, $^{4}J$(H,H) = 1.2 Hz, 2H; H3 thienyl), 7.13 (dd, $^{3}J$(H,H) = 5.1 Hz, $^{4}J$(H,H) = 1.2 Hz, 2H; H5 thienyl); $^{13}$C{$^{1}$H} NMR (75 MHz, $\mathrm{CDCl_3}$): $\delta = 19.3$ (s, $\mathrm{C{\equiv}CCH_2}\mathit{C}\mathrm{H_2}$), 19.4 (s, $\mathrm{C{\equiv}CCH_2}\mathit{C}\mathrm{H_2}$), 27.7 (s, $\mathrm{C{\equiv}C}\mathit{C}\mathrm{H_2}$), 27.8 (s, $\mathrm{C{\equiv}C}\mathit{C}\mathrm{H_2}$), 74.1 (s, $\mathit{C}\mathrm{{\equiv}CCS}$), 74.2 (s, $\mathit{C}\mathrm{{\equiv}C\text{-}C\text{-}S}$), 93.8 (s, $\mathrm{C{\equiv}}\mathit{C}\mathrm{CS}$), 95.4 (s, $\mathrm{C{\equiv}}\mathit{C}\mathrm{CS}$), 123.2 (s, C2′ thienyl), 123.5 (s, C4′ thienyl), 124.1 (s, C2 thienyl), 126.1 (s, C5 thienyl), 126.8 (s, C4 thienyl), 131.0 (s, C3 thienyl), 131.0 (s, C3′ thienyl), 137.0 (s, C5′ thienyl); HR-MS (FAB, *m*-NBA): *m*/*z*: 538.09190 $[M]^+$; calcd for $\mathrm{C_{32}H_{26}S_4}$: 538.09174; elemental analysis (%) calcd for $\mathrm{C_{32}H_{26}S_4}$ (538.80): C 71.34, H 4.86; found: C 71.01, H 4.98.

**Mixed phosphole–thiophene oligomer 11**: Following the procedure described for compound **3a**, reaction of **10** (0.115 g, 0.21 mmol), $[\mathrm{Cp_2ZrCl_2}]$ (0.125 g, 0.42 mmol), *n*BuLi (1.6 M, 0.58 mL, 0.94 mmol) and $\mathrm{PhPBr_2}$ (0.097 mL, 0.47 mmol) afforded the $\sigma^3$-phosphole derivative after filtration on basic alumina ($^{31}$P{$^{1}$H) NMR (81 MHz, $\mathrm{CDCl_3}$): $\delta = +11.5$). Elemental sulfur (0.018 g, 0.07 mmol) was added to this THF solution. The reaction mixture was stirred for 36 h at room temperature and filtered, and the solvent was removed in vacuo. After purification on silica gel ($\mathrm{Et_2O}$/heptane 20:80), **11** was obtained as an orange solid (yield: 0.04 g, 0,05 mmol, 23 %). $R_f = 0.15$ (silica gel, $\mathrm{Et_2O}$/heptane 20:80); $^{1}$H NMR (200 MHz, $\mathrm{CDCl_3}$): $\delta = 1.90$ (m, 8H; $\mathrm{C{=}CCH_2}\mathit{CH_2}$), 2.90 (m, 8H; $\mathrm{C{=}C}\mathit{CH_2}$), 6.95 (m, 4H; H4, H4′ thienyl), 7.28 (m, 4H; H5, H3 thienyl), 7.38 (m, 8H; H3′ thienyl, *m*-/*p*-H Ph), 7.86 (m, 4H; *o*-H Ph); $^{13}$C{$^{1}$H) NMR (75 MHz, $\mathrm{CDCl_3}$): $\delta = 21.7$ (s, $\mathrm{C{=}CCH_2}\mathit{C}\mathrm{H_2}$), 28.4 (s, $\mathrm{C{=}C}\mathit{C}\mathrm{H_2}$), 123.2 (s, C4′ thienyl), 125.8 (s, C5 thienyl), 126.4 (s, C4 thienyl), 126.7 (d, $^{3}J$(P,C) = 5.8 Hz, C3 thienyl), 127.8 (s, C3′ thienyl), 127.9 (d, $^{3}J$(P,C) = 12.6 Hz, *m*-C Ph), 129.6 (d, $^{2}J$(P,C) = 11.7 Hz, *o*-C Ph), 131.1 (d, $^{4}J$(P,C) = 2.5 Hz, *p*-C Ph), 133.4 (d, $^{2}J$(P,C) = 18.1 Hz, C2 or C2′ thienyl), 133.6 (d, $^{2}J$(P,C) = 17.1 Hz, C2 or C2′ thienyl), 137.1 (s, C5′ thienyl), 143.9 (d, $^{2}J$(P,C) = 20.1 Hz, $\mathrm{PC{=}}\mathit{C}$), 144.2 (d, $^{2}J$(P,C) = 21.3 Hz, $\mathrm{PC{=}}\mathit{C}$), $\mathrm{P}\mathit{C}\mathrm{{=}C}$ and ipso-C Ph were not observed; $^{31}$P{$^{1}$H) NMR (81 MHz, $\mathrm{CDCl_3}$): $\delta = +52{,}6$; HR-MS (FAB, *m*-NBA): *m*/*z*: 818.0614 $[M]^+$; calcd for $\mathrm{C_{32}H_{26}S_4}$: 818.06166; elemental analysis (%) calcd for $\mathrm{C_{44}H_{36}S_6P_2}$ (818.06): C 64.54, H 4.44; found: C 64.21, H 4.30.

## Acknowledgements

This work was financially supported by the Conseil Régional Bretagne, the Ministère de l'Education Nationale, de la Recherche et de la Technologie and the Centre National de la Recherche Scientifique. Support of the Hungarian Ministry of Education FKFP 0029/2000 is also acknowledged.

---

[1] Recent reviews: a) A. Kraft, A. C. Grimsdale, A. B. Holmes, *Angew. Chem.* **1998**, *110*, 416–443; *Angew. Chem. Int. Ed.* **1998**, *37*, 403–428; b) K. Müllen, G. Wegner, *Electronic Materials*: *The Oligomer Approach*, Wiley-VCH, Weinheim, **1998**; c) *Handbook of Conducting Polymers* (Eds.: T. A. Skotheim, R. L. Elsenbaumer, J. R. Reynolds), Marcel Dekker, New York, 1998; d) J. Roncali, *Chem. Rev.* **1997**, *97*, 173–205; e) F. Garnier, *Acc. Chem. Res.* **1998**, *32*, 209–215; f) J. M. Tour, *Acc. Chem. Res.* **2000**, *33*, 791–804; g) U. Mitschke, P. Bäuerle, *J. Mater. Chem.* **2000**, *10*, 1471–1507; h) J. L. Segura, N. Martin, *J. Mater. Chem.* **2000**, *10*, 2403–2435; i) R. E. Martin, F. Diederich, *Angew. Chem.* **1999**, *111*, 1440–1469; *Angew. Chem. Int. Ed.* **1999**, *38*, 1350–1377; j) F. Fichou, *J. Mater. Chem.* **2000**, *10*, 571–588; For recent contributions, see k) T-Q. Nguyen, J. Wu, V. Doan, B. J. Schwartz, S. H. Tolbert, *Science* **2000**, *288*, 652–656; l) M. A. Baldo, M. E. Thompson, S. R. Forrest, *Nature* **2000**, *403*, 750–752; m) Y. Shi, C. Zhang, H. Zhang, J. H. Bechtel, L. R. Dalton, B. H. Robinson, W. H. Steier, *Science* **2000**, *288*, 119–122.

[2] a) D. J. Irvin, C. J. Dubois, J. R. Reynolds, *Chem. Commun.* **1999**, 2121–2122; b) Z. Zhou, T. Maruyama, T. Kanbara, T. Ikeda, K. Ichimura, T. Yamamoto, K. Tokuda, *J. Chem. Soc. Chem. Commun.* **1991**, 1210–1212; c) T. Yamamoto, Z.-H. Zhou, T. Kanbara, M. Shimura, K. Kizu, T. Maruyama, Y. Nakamura, T. Fukuda, B. L. Lee, N. Ooba, S. Tomura, T. Kurihara, T. Kaino, K. Kubota, S. Sasaki, *J. Am. Chem. Soc.* **1996**, *118*, 10389–10399; d) Q. T. Zhang, J. T. Tour, *J. Am. Chem.Soc.* **1998**, *120*, 5355–5362; e) C.-F. Lee, L.-M.Yang, T.-Y. Hwu, A.-S. Feng, J.-C. Tseng, T.-Y. Luh, *J. Am. Chem. Soc.* **2000**, *122*, 4992–4993; f) I. Albert, T. Marks, M. Ratner, *J. Am. Chem. Soc.* **1997**, *119*, 6575–6582; g) B. Jiang, T. D. Tilley, *J. Am. Chem. Soc.* **1999**, *121*, 9744–9745; h) M. C. Suh, B. Jiang, T. D. Tilley, *Angew. Chem.* **2000**, *112*, 2992–2995; *Angew. Chem. Int. Ed.* **2000**, *39*, 2870–2873; i) S. Yamagushi, Y. Itami, K. Tamao, *Organometallics* **1998**, *17*, 4910–4916; j) S. Yamagushi, T. Endo, M. Uchida, T. Izumizawa, K. Furukawa, K. Tamao, *Chem. Eur. J.* **2000**, *6*, 1683–1692; k) S. Yamagushi, T. Goto, K. Tamao, *Angew. Chem.* **2000**, *112*, 1761–1763; *Angew. Chem. Int. Ed.* **2000**, *39*, 1695–1697; l) K. Tamao, S. Yamagushi, M. Shiozaki, Y. Nakagawa, Y. Ito, *J. Am. Chem. Soc.* **1992**, *114*, 5867–5869; m) S. Yamagushi, K. Tamao, *J. Chem. Soc. Dalton Trans.* **1998**, 3693–3702;

n) R. J. P. Corriu, W. E. Douglas, Z.-X Yang, *J. Organomet. Chem.* **1993**, *456*, 35–39; o) J. P. Ferraris, R. G. Andrus, D. C. Hrncir, *J. Chem. Soc. Chem. Commun.* **1989**, 1318–1320; p) A. Hucke, M. P. Cava, *J. Org. Chem.* **1998**, *63*, 7413–7417; q) B. L. Lucht, M. A. Buretea, T. D. Tilley, *Organometallics*, **2000**, *19*, 3469–3475.

[3] a) F. Mathey, *Chem. Rev.* **1988**, *88*, 429–453; b) L. D. Quin in *Comprehensive Heterocyclic Chemistry* (Ed.: A. R. Katritzky), Pergamon, Oxford, **1996**, pp. 757–856.

[4] a) E. Deschamps, L. Ricard, F. Mathey, *Angew. Chem.* **1994**, *106*, 1214–1217; *Angew. Chem. Int. Ed. Engl.* **1994**, *33*, 1158–1161; b) M.-O. Bevière, F. Mercier, L. Ricard, F. Mathey, *Angew. Chem.* **1990**, *102*, 672–675; *Angew. Chem. Int. Ed. Engl.* **1990**, *29*, 655–657; c) M-O Bévierre, F. Mercier, F. Mathey, A. Jutand, C. Amatore, *N. J. Chem.* **1991**, *15*, 545–550; d) This assumption, proposed by the authors themselves, is supported by the fact that the C–C inter-ring bonds of quaterphospholes are not shortened; e) S. S. H. Mao, T. D. Tilley, *Macromolecules* **1997**, *30*, 5566–5569.

[5] a) U. Salzner, J. B. Lagowski, P. G. Pickup, R. A. Poirier, *Synth. Met.* **1998**, *96*, 177–189; b) D. Delaere, A. Dransfeld, M. N. Nguyen, L. G. Vanquickenborne, *J. Org. Chem.* **2000**, *65*, 2631–2636; c) L. Nyulazi, T. Vespremi, J. Réffy, B. Burhardt, M. Regitz, *J. Am. Chem. Soc.* **1992**, *114*, 9080–9084; d) P. von R. Schleyer, C. Maerker, A. Dransfeld, H. Jiao, N. J. R. von Eikema Hommes, *J. Am. Chem. Soc.* **1996**, *118*, 6317–6318; e) P. von R. Schleyer, P. K. Freeman, H. Jiao, B. Goldfuss, *Angew. Chem.* **1995**, *107*, 332–335; *Angew. Chem. Int. Ed. Engl.* **1995**, *34*, 337–340; f) B. D. Chesnut, L. D. Quin, *J. Am. Chem. Soc.* **1994**, *116*, 9638–9643; g) A. Dransfeld, L. Nyulaszi, P. von R. Schleyer, *Inorg. Chem.* **1998**, *37*, 4413–4420; h) E. Mattmann, D. Simonutti, L. Ricard, F. Mercier, F. Mathey, *J. Org. Chem.* **2001**, *66*, 755–758; i) G. Keglevich, L. D. Quin, Z. Böcskei, G. M. Keserü, R. Kalgutkar, P. M. Lahti, *J. Organomet. Chem.* **1997**, *532*, 109–116; j) G. Keglevich, T. Chuluunbaatar, B. Dajka, A. Dobó, A. Szöllösy, L. Töke, *J. Chem. Soc. Perkin Trans. 1* **2000**, 2895–2897; k) L. Nyulászi, *Chem. Rev.* **2001**, *101*, 1229–1246.

[6] a) P. J. Fagan, W. A. Nugent, *J. Am. Chem. Soc.* **1988**, *110*, 2310–2312; b) P. J. Fagan, W. A. Nugent, J. C. Calabrese, *J. Am. Chem. Soc.* **1994**, *116*, 1880–1889; c) X. Sava, N. Mézaille, N. Maigrot, F. Nief, L. Ricard, F. Mathey, P. Le Floch, *Organometallics* **1999**, *18*, 4205–4215; d) E. Negishi, T. Takahashi, *Acc. Chem. Res.* **1994**, *27*, 124–130; e) T. Takahashi, F.-Y. Tsai, Y. Li, K. Nakajima, M. Kotora, *J. Am. Chem. Soc* **1999**, *121*, 11093–11100.

[7] It is well known that hydrolysis of zirconacyclopentadienes affords the corresponding diene and zirconium oxides: B. L. Lucht, T. D. Tilley, *Chem. Commun.* **1998**, 1645–1646.

[8] a) W. N. Nugent, D. L. Thorn, R. L. Harlow, *J. Am. Chem. Soc.* **1987**, *109*, 2788–2796; b) W. E. Hunter, J. L. Atwood, G. Fachinetti, C. Floriani, *J. Organomet. Chem.* **1981**, *204*, 67–74; c) K. Oouchi, M. Mitani, M. Hayakawa, T. Yamada, T. Mukaiyama, *J. Organomet. Chem.* **1996**, *516*, 111–114.

[9] a) D. Le Vilain, C. Hay, V. Deborde, L. Toupet, R. Reau, *Chem. Commun.* **1999**, 345–346; b) C. Hay, C. Fishmeister, M. Hissler, L. Toupet, R. Réau, *Angew. Chem.* **2000**, *112*, 1882–1885; *Angew. Chem. Int. Ed.* **2000**, *39*, 1812–1815.

[10] a) R. E. Niziurski, C. C. Scordilis-Kelley, T. L. Liu, M. P. Cava, R. T. Carlin, *J. Am. Chem. Soc.* **1993**, *115*, 887–891; b) G. Barbarella, M. Zambianchi, L. Antolini, P. Ostoja, P. Maccagnari, A. Bongini, E. A. Marseglia, E. Tedesco, G. Gigli, R. Cingolani, *J. Am. Chem. Soc.* **1999**, *121*, 8920–8926, and references therein.

[11] a) C. Reichardt, *Chem. Rev.* **1994**, *94*, 2319–2358; b) M. J. Kamlet, J. L. M. Abboud, M. H. Abraham, R. W. Taft, *J. Org. Chem.* **1983**, *48*, 2877–2887.

[12] a) P. Audebert, J.-M. Catel, G. Le Coustumer, V. Duchenet, P. Hapiot, *J. Phys. Chem. B* **1998**, *102*, 8661–8669; b) P. Audebert, J.-M. Catel, V. Duchenet, L. Guyard, P. Hapiot, G. Le Coustumer, *Synth. Met.* **1999**, *101*, 642–645; c) R. Michalitsch, A. El Kassmi, A. Yassar, P. Lang, F. Garnier, *J. Electroanal. Chem.* **1998**, *457*, 129–139; d) S. Y. Hong, *Chem. Mater.* **2000**, *12*, 495–500; e) S. Tanaka, M. Kumei, *J. Chem. Soc. Chem. Commun* **1995**, 815–816; J. Roncali, F. Garnier, M. Lemaire, R. Garreau, *Synth. Met.* **1986**, *15*, 323; f) F. Demanze, P. Godillot, F. Garnier, P. Hapiot, *J. Electroanal. Chem.* **1996**, *414*, 61–67; c) P. Audebert, J.-M. Catel, G. Le Coustumer, V. Duchenet, P. Hapiot, *J. Phys. Chem.* **1995**, *99*, 11923–11929.

[13] J. W. Hershberger, R. J. Klinger, J. K. Kochi, *J. Am. Chem. Soc.* **1982**, *104*, 3034–3043.

[14] R. E. Niziurski, C. C. Scordilis-Kelley, T. L. Liu, M. P. Cava, R. T. Carlin, J. P. Ferraris, *J. Am. Chem. Soc.* **1993**, *115*, 887–891.

[15] T. Yamamoto, K. Sugiyama, T. Kushida, T. Inoue, T. Kanbara, *J. Am. Chem. Soc.* **1996**, *118*, 3930–3937.

[16] a) K. Tamao, M. Uchida, T. Izumizawa, K. Furukawa, S. Yamaguchi, *J. Am. Chem. Soc.* **1996**, *118*, 11974–11975; b) M. Strukelj, F. Papadimitrakopoulos, T. M. Miller, L. J. Rothberg, *Science*, **1995**, *267*, 1969–1972; c) M. Strukelj, T. M. Miller, F. Papadimitrakopoulos, S. Son, *J. Am. Chem. Soc.* **1995**, 117, 11976–11983.

[17] a) B. L. Lucht, N. O. St. Onge, *Chem. Commun.* **2000**, 2097–2098; b) N. Matsumi, K. Naka, Y. Chujo, *J. Am. Chem. Soc.* **1998**, 120, 10776–10777; c) G. Barbarella, L. Favaretto, G. Sotgiu, M. Zambianchi, L. Antolini, O. Pudova, A. Bongini, *J. Org. Chem.* **1998**, *63*, 5497–5506;

[18] a) S. Yamaguchi, R.-Z. Jin, K. Tamao, F. Sato, *J. Org. Chem.* **1998**, *63*, 10060–10062; b) L. D. Quin, J. P. Gratz, T. P. Barket, *J. Org. Chem.* **1968**, *33*, 1034–1041; c) W. P. Jackson, *Synlett* **1990**, *9*, 493; d) R. M. Kellogg, A. P. Schaap, H. Wynberg, *J. Org. Chem.* **1969**, *34*, 343–346.

[19] J. N. Demas, G. A. Crosby, *J. Phys. Chem.* **1971**, *75*, 991–1024.

[20] J. Rault-Berthelot, V. Questaigne, J. Simonet, G. Peslerbe, *New J. Chem.* **1989**, *13*, 45–52.

[21] M. J. Frisch, G. W. Trucks, H. B. Schlegel, G. E. Scuseria, M. A. Robb, J. R. Cheeseman, V. G. Zakrzewski, J. A. Montgomery, R. E. Stratmann, J. C. Burant, S. Dapprich, J. M. Millam, A. D. Daniels, K. N. Kudin, M. C. Strain, O. Farkas, J. Tomasi, V. Barone, M. Cossi, R. Cammi, B. Mennucci, C. Pomelli, C. Adamo, S. Clifford, J. Ochterski, G. A. Petersson, P. Y. Ayala, Q. Cui, K. Morokuma, D. K. Malick, A. D. Rabuck, K. Raghavachari, J. B. Foresman, J. Cioslowski, J. V. Ortiz, B. B. Stefanov, G. Liu, A. Liashenko, P. Piskorz, I. Komaromi, R. Gomperts, R. L. Martin, D. J. Fox, T. Keith, M. A. Al-Laham, C. Y. Peng, A. Nanayakkara, C. Gonzalez, M. Challacombe, P. M. W. Gill, B. G. Johnson, W. Chen, M. W. Wong, J. L. Andres, M. Head-Gordon, E. S. Replogle, J. A. Pople, Gaussian 98 (Revision A.5), Gaussian, Pittsburgh, PA, **1998**..

[22] a) C. K. Fair, MolEN, An Interactive Intelligent System for Crystal Structure Analysis, User Manual, Enraf-Nonius, Delft (The Netherlands), **1990**; b) A. L. Spek, HELENA, Program for the Handling of CAD4-Diffractometer Output, SHELX(S/L), Utrecht University, Utrecht (The Netherlands), **1997**; c) A. Altomare, M. C. Burla, M. Camalli, G. Cascarano, C. Giacovazzo, A. Guagliardi, A. G. G. Moliterni, G. Polidori, R. Spagna, *J. Appl. Crystallogr.* **1998**, *31*, 74–77; d) G. M. Sheldrick, SHELX97-2, Program for the Refinement of Crystal Structures, Universität Göttingen (Germany), **1998**; e) *International Tables for X-ray Crystallography, Vol. C* (Ed.: A. J. C. Wilson), Kluwer, Dordrecht, **1992**; f) A. L. Spek, PLATON, A Multipurpose Crystallographic Tool, Utrecht University, Utrecht (The Netherlands), **1998**.

Received: April 6, 2001 [F3180]